DISSERTATION

ESSAYS ON BITCOIN MINING AND RENEWABLE ENERGY: EXPLORING SUSTAINABILITY AND PROFITABILITY

Submitted by

Simon Poltak Hamonangan Hutabarat

Department of Economics

In partial fulfillment of the requirements

For the Degree of Doctor of Philosophy

Colorado State University

Fort Collins, Colorado

Summer 2023

Doctoral Committee:

Advisor: Terrence Iverson

Anders Fremstad
Martin Shields
Jesse Burkhardt

ABSTRACT

ESSAYS ON BITCOIN MINING AND RENEWABLE ENERGY: EXPLORING SUSTAINABILITY AND PROFITABILITY

This Ph.D. dissertation comprises three interlinked studies exploring the intersection of renewable energy economics and cryptocurrency mining, focusing on Bitcoin. Using data from the California Independent Service Operator (CAISO) and a case study from East Indonesia, this research aims to inform energy and financial policies for a sustainable future. The first chapter, "Harnessing Renewable Energy for Cryptocurrency Mining: An Analysis of Locational Marginal Prices in California," looks into the potential of Bitcoin mining to utilize the surplus renewable energy produced during daylight hours when demand is relatively low. It considers whether the Locational Marginal Prices (LMPs) are systematically lower in areas rich in renewable energy resources, presenting an opportunity for strategic Bitcoin mining operations. The second chapter, "Assessing the Impact of Bitcoin Prices on Optimal Mining Hours: Implications for Renewable Energy Development," explores the profitability dynamics of Bitcoin mining. The study discusses the influence of Bitcoin prices and electricity costs on mining operations' profitability, including the ideal hours of operation. The findings suggest that for Bitcoin to be "green" and reduce carbon emissions, the Bitcoin price must be significantly lower than historical averages. The final chapter, "Exploring the Effects of Production Tax Credits on Renewable Energy Development: A Computable General Equilibrium Approach in East Indonesia," evaluates the potential impact of production tax credits (PTCs) on Indonesia's renewable energy industry. This study provides a quantitative assessment of the economic implications of a PTC, contributing to the ongoing debate on incentivizing renewable energy development. Together, these chapters offer insights into the potential of cryptocurrency

mining to harness renewable energy, the factors affecting the profitability of Bitcoin mining, and the impact of tax incentives on renewable energy development. These findings could guide policymakers and stakeholders in making informed decisions for a sustainable and profitable future.

ACKNOWLEDGEMENTS

First and foremost, I want to express my deepest gratitude to my Lord and Savior, Jesus Christ. Without His love, grace, and divine guidance, this journey would have been impossible. His presence in my life has provided strength, inspiration, and unwavering faith, allowing me to overcome challenges and persevere through every step of this dissertation.

I sincerely appreciate my extraordinary supervisor and mentor, Dr. Terrence (Terry) Iverson. His unwavering support, boundless enthusiasm, and sage advice have been the compass guiding me through the labyrinth of academia. His ability to challenge my ideas while nurturing my growth has been inspiring.

I am also indebted to the members of my dissertation committee, Dr. Anders Fremstad, Dr. Martin Shields, and Dr. Jesse Burkhardt. Their expertise and thoughtful contributions have significantly enriched this study and expanded my understanding of energy economics.

To the faculty and staff at the Department of Economics at Colorado State University, thank you for fostering an environment where curiosity thrives and knowledge blossoms. Your commitment to excellence and unwavering support has been instrumental in realizing this dissertation.

Additionally, I want to express my heartfelt gratitude to my family and friends for their unwavering support, encouragement, and understanding throughout this journey. Their love, motivation, and belief in my abilities have been the driving force behind my accomplishments.

Finally, I extend my heartfelt appreciation to all who supported and inspired me throughout this dissertation journey. Your collaborative spirit enriched this study. Special thanks to Indonesia's Directorate General of Taxes Ministry of Finance and The Indonesia Endowment Funds for Education (LPDP) for their invaluable support.

DEDICATION

To my beloved family—my father, Sabam Hutabarat; my mother, Berliana Sibuea; and my two brothers, Stefan Hutabarat and Samuel Hutabarat—I dedicate this dissertation. Your unwavering presence and boundless love have been the driving force behind my pursuit of knowledge. In the vast universe of academia, our familial bond transcends space and time, anchoring me with strength and inspiration. This work is a testament to our shared journey and the endless possibilities that unfold when we stand united.

TABLE OF CONTENTS

LIST OF TABLES

LIST OF FIGURES

Chapter 1

Harnessing Renewable Energy for Cryptocurrency Mining: An Analysis of Locational Marginal Prices in California

1.1 Introduction

Bitcoin mining has become a major industry in recent years, with an estimated 4 million active miners worldwide. However, the process of verifying transactions on the blockchain network requires a significant amount of computational power, leading to a corresponding increase in energy consumption. In fact, it has been estimated that Bitcoin mining consumes more energy than entire countries such as Argentina[1] or Sweden. It has led to concerns about the environmental impact of Bitcoin mining, particularly given the global push towards renewable energy sources to combat climate change.

In this context, the argument that Bitcoin may contribute to reducing carbon dioxide emissions through its complementary relationship with renewable energy is intriguing and potentially significant. By taking advantage of off-peak renewable electricity, Bitcoin mining could lessen the need for fossil fuel-based power generation during peak demand hours, ultimately decreasing carbon emissions.

Energy usage from Bitcoin mining has exploded in recent years, reaching almost one percent of global electricity demand in 2021. Despite the large energy usage, Jack Dorsey, Elon Musk, and others have argued that Bitcoin may actually serve to lower carbon dioxide

[1] Argentina's economic challenges, including high inflation rates and capital controls, have led to a surge in cryptocurrency mining. The country's low electricity costs, driven by residential subsidies and a favorable exchange rate, have attracted miners seeking profitability. This trend gains significance in light of China's recent ban on cryptocurrency mining, which has prompted miners to explore alternative locations such as Argentina.

emissions. The argument stems from the assumption that Bitcoin is complementary to renewable energy. In particular, because Bitcoin only requires short bursts of continuous energy to compete in the rolling sequence of 10-minute tournaments, it can, in principle, take advantage of off-peak renewable electricity in a way that conventional economic activities cannot.

Research questions. The research questions addressed in this paper are:

RQ1. What are the cheapest Locational Marginal Prices (LMPs) per hour based on California Independent Service Operator data? Because Bitcoin doesn't need continuous electricity, just a ten-minute spurt of electricity, the nature of renewable energy is that its supply is intermittent, meaning that it comes in spurts. For most economic activities, this is a disadvantage, but not for Bitcoin mining. Because much renewable energy comes during the day with limited use, the spot price of electricity is low and could be productively used to mine Bitcoin;

RQ2. Is there evidence that LMPs are systematically lower in the vicinity of renewables? Considering this question, I am interested in more than average daily prices. I also want to consider the extent to which prospective Bitcoin miners can benefit from selectively running mining operations during select portions of the day.

This research has important implications for understanding the potential role of Bitcoin mining in the transition toward a more sustainable energy system. By shedding light on the relationship between Bitcoin mining and renewable energy, I hope to contribute to the broader conversation around sustainable energy solutions and inform policy decisions related to energy and environmental sustainability.

To assess the plausibility of this claim, this chapter uses data on real-time electricity pricing from the CAISO electricity grid. Specifically, prospective Bitcoin miners may benefit from deliberately locating in the vicinity of renewable energy facilities to access cheaper electricity prices. By analyzing Locational Marginal Prices (LMPs) based on CAISO data from 2018-2020, I investigate whether there is evidence that LMPs are systematically lower in the vicinity of renewables. In doing so, I look beyond average daily prices and consider the cheapest hours of the day by facility and by generation type.

Analyzing the hourly dynamics of Locational Marginal Prices (LMPs) provides valuable insights into the intricate dynamics of electricity pricing. By examining the variations in LMPs throughout a 24-hour observation period, I can uncover patterns and trends that shed light on the factors driving pricing fluctuations. In this analysis, I focused on the contributions of different power sources, including biogas/biomass, coal, geothermal, natural gas, sun, uranium, water, and wind, to LMPs during specific hours. My findings highlight the importance of renewable energy sources such as wind, sun, geothermal, and water in driving down prices, particularly during the early hours of the day. These insights can inform strategic decision-making for collocating Bitcoin mining operations near renewable energy sources, optimizing energy efficiency, and reducing operational expenses.

This paper has five sections. In the next section, I will describe the theoretical foundation of the economics of LMPs. In section 1.3, I will summarize the statistics of CAISO datasets from 2018 to 2020 and build the econometric models. Then, I will present and interpret the results in section 1.4. Finally, Section 1.5 is the conclusion based on the results found in section 1.4.

1.2 Previous studies

Several studies looked at the role of the analysis of electricity prices to analyze energy economics issues. For example, Fell et al. (2021) revealed that by using only wind data for regression from the SPP RTO along with the emission data (CO2, NO2), they are able to quantify the effect of decarbonization using renewable energy. Burkhardt et al. (2019) conducted the experimental field evidence on the effects of information and pricing on residential electricity conservation using datasets from ERCOT, 200 million, similar to CAISO.

Furthermore, the issues of negative wholesale electricity prices have been associated with oversupply, which is the marginal generator would prefer to pay the price rather than reduce its output. Seel et al. (2021) studied that in 2020, negative real-time hourly wholesale prices occurred in about 4 % of all hours and wholesale market nodes (out of > 50,000 nodes) across the United States. Regional clusters have emerged, for example, in the wind-rich central plains, where production tax incentives delay wind energy curtailment even as prices turn negative. Negative prices can occur at individual pricing nodes or clusters of nodes when transmission capacity is insufficient to export electricity to demand centers or widespread across an entire market.

In addition, according to Papageorgiou et al. (2021), the storage device could buy power at night and sell it during the day. That is due to providing energy, ancillary services, and capacity in regions with a lot of wind generation at night. Depending on the technology, this price arbitrage process can occur several times during the day. Also, it can release energy for short or long periods, store it for multiple days, and release it gradually when prices are high.

Antweiler (2021) finds that system operators have adopted curtailment protocols without a market mechanism to prevent oversupply. When intermittent power producers receive fixed feed-in-tariffs (FIT), they will continue to bid into the market just above the negative value of the FIT and still make a profit.

The science journal (German Day-Ahead Energy Market, 2018) [2] explains how the negative prices come up in the first place. Figure 1.1a shows that Power producers bid certain amounts of power for a specific price, while buyers lodge into the order book how much power they are willing to buy at a given price. That is done by noon for all hours of the following day. On the other hand, Figure 1.1b shows that negative power prices on the electricity exchange occur when a high and inflexible power generation appears simultaneously with low electricity demand. Power producers offer their electricity for

[2] Retrieved from https://www.cleanenergywire.org/factsheets/why-power-prices-turn-negative

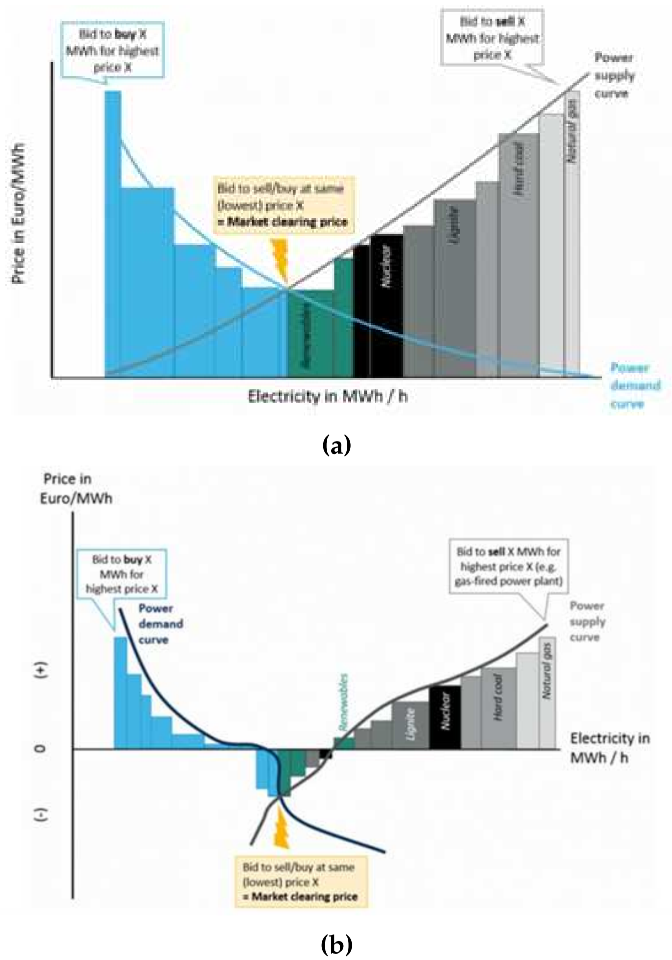

Figure 1.1: The supply and demand curve in the energy market (Source: German Day-Ahead Energy Market, 2018)

negative prices on the exchange, particularly in hours of (predictable) high renewable power supply (lots of wind and sun).

This paper will contribute to the literature as follows. First, the effect of negative LMPs would be significant to the cryptocurrency miners whether they decide to benefit from the renewable energy colocation. Second, there are possibilities to stay mining during a particular time of the day when renewables, like wind and solar power, can be utilized for cryptocurrency mining.

1.3 Empirical evidence

In this section, I analyze a comprehensive dataset obtained from the California Independent Service Operator (CAISO) and the US Energy Information Administration (EIA). My focus is on examining the California region's Locational Marginal Prices (LMP) from 2018 to 2020. The dataset encompasses key variables such as hour, LMP, and category, which respectively represent the generator ID, electricity prices throughout the day, and the energy source of power plants.

Initially, the dataset consisted of 27,079,105 observations. However, I refined it to cover the time frame from January 1, 2018, to December 31, 2020, resulting in 27,078,020 observations that are now ready for analysis. Table 1.1 comprehensively overviews the dataset's construction and highlights the data sources involved.

Table 1.1: Construction of the datasets

Procedures	Remaining Amount of Data	Notes
Original datasets	27,079,105	Retrieving from the CAISO website
Reduction due to the 2017 exclusion	27,078,020	Cleanup for only 2018-2020 datasets
Nighttime Solar observation removal	26,489,618	Drop the Solar observation from 6 AM to 6 PM

Source: Author's Calculation

It is important to note that my analysis solely focuses on CAISO data and does not incorporate transmissions from other operators. The code follows CAISO's established methodology to ensure consistency and adherence to industry standards. In the subsequent section, I present summary statistics that reveal insights into the average n-cheapest hours of LMPs for eight specific power sources of interest.

The CAISO data provides hourly LMP data for different nodes/generators within a day. The key variables in the dataset are node or Generator ID (the generator ID corresponds to the power plant), *year* (the year of observation, i.e., 2018 to 2020), *month* (the month of observation, coded as 1 for January to 12 for December), *day* (the day of observation, coded as 1 to 31, 1 to 30, 1 to 28, or 29), *hour* (hourly data ranging from 1 to 24), *LMP* (the Locational Marginal Price in \$/MWh), and category or Resource ID (8 power sources observed: wind, sun, biogas/biomass, uranium, natural gas, coal, geothermal, and water). The Locational Marginal Price (LMP) is a measure that represents the electricity price at different locations and times within a given month and year. It is calculated by considering several factors: the marginal cost of energy (MCE), the marginal congestion cost (MCC), and the marginal cost loss (MCL).

The MCE reflects the cost of generating an additional unit of electricity at a specific location and time. The MCC accounts for the additional cost incurred due to congestion in the transmission system, which occurs when the electricity demand exceeds the available transmission capacity. The MCL represents the cost associated with electrical losses during electricity transmission.

To determine the LMP, I subtract the MCL from the sum of the MCE and MCC. This subtraction is necessary to account for the costs associated with electrical losses and congestion, subtracted from the overall value to obtain the final LMP.

It's important to note that while the MCL can sometimes be negative, the LMP itself is not necessarily negative. The LMP can take positive, negative, or zero values depending on supply and demand conditions, generation costs, and transmission constraints. The LMP values provide information about real-time electricity pricing at specific locations, facilitating efficient market operations and grid management.

However, it is worth noting that approximately 20% of the nodes exhibit a situation where multiple power plants are connected to them. In simpler terms, these nodes receive electricity from various sources, benefitting from a diverse power generation network. Instead of relying on a single power plant, these locations draw electricity from multiple sources, contributing to a reliable and stable electricity supply. Understanding this phenomenon offers valuable insights into the collaborative efforts of various energy sources in meeting the energy demands of these nodes.

For instance, let's consider a scenario where a node is connected to a gas-fired and solar power plant. These two plants generate electricity from different resources, resulting in distinct pricing dynamics for each plant at that specific node. As a result, the market reflects different prices for the electricity produced by each plant. It is important to understand that overnight prices for nodes near solar plants are not a mistake or anomaly.

During nighttime periods when solar plants are not actively generating electricity, the listed price at that node represents the compensation the gas-fired power plant would receive for its electricity production. Conversely, when the solar plant can generate electricity during daylight hours, the listed price corresponds to the value it would receive for its output. This differentiation in prices allows for a fair and accurate representation of the contribution of each power plant to the electricity market at that node.

Moreover, this pricing mechanism has implications for load-serving entities procuring node power. If a load-serving entity purchases electricity from the gas-fired power plant at that node, it will pay the listed price associated with the gas generator's electricity production. On the other hand, if they procure electricity from the solar plant, they would pay the listed price associated with that specific plant.

Overall, this explanation demonstrates how the presence of multiple power plants connected to a single node introduces variations in the pricing and reflects the diverse mix of energy sources involved in supplying electricity to that location. By accurately assigning prices based on the specific plant's electricity production, the market ensures fairness and transparency in the compensation and procurement processes. These insights shed light on the complex dynamics of my electricity supply system, showcasing the collaborative efforts of different energy sources in meeting my energy needs efficiently and sustainably.

One issue that arose in the data is that there were several instances of nighttime prices for solar. Since these must reflect non-solar generation, I decided to drop these observations throughout. That doesn't completely eliminate the concern about imprecisely identifying the resource at each location, but it at least goes part of the way toward doing so. Table 1.2

highlights the pricing implications for load-serving entities procuring power from nodes with multiple power sources.

Table 1.2: Power Plant and Generated Electricity Source for Nodes with Multiple Power

Power Plant code name	Generated Electricity Source	Notes
COGNTNL_7_B1	Coal, Biogas/Biomass	Depending on the source, entities will pay the listed price associated with the respective generator, whether it be gas-fired or coal-fired, reflecting the diverse pricing dynamics within the market.
CPCSTCN_7_B1	Coal, Biogas/Biomass	
LASSEN_6_N003	Natural Gas, Biogas/Biomass	
MISSION_2_N035	Natural Gas, Water	
MTPOSO_7_N001	Coal, Biogas/Biomass	
SCLARA_6_N008	Natural Gas, Biogas/Biomass, Water	

Source: Author's Calculation

In the context of CAISO datasets, "resource ID" refers to a unique identifier assigned to individual power generation resources or energy storage systems participating in the electricity market. This identifier helps in tracking and distinguishing different resources within the dataset.

LMPs (Locational Marginal Prices) are wholesale electricity prices at specific locations within the power grid. They represent the cost of producing one additional unit of electricity at a particular location and time. LMPs are determined through market mechanisms such as auctions and reflect the supply and demand conditions in real-time or day-ahead markets.

Each resource participating in the market is assigned a resource ID to determine LMPs in the CAISO datasets. This ID allows CAISO to track and attribute the generation or consumption of electricity to specific resources. By associating the LMP values with resource IDs, CAISO can provide detailed information about pricing at different locations and analyze the performance of individual resources in the electricity market.

It is also important to note that the variable LMP from the corresponding category, such as sun, wind, etc., is likely derived from the vicinity of each node. For example, all the LMP data for hours (n = 1, ..., 24) from wind or solar generators are explicitly generated from the associated generators. Therefore, there is no electricity spillover from different power sources that "leak" into one another.

1.3.1 Summary statistics of nodes

This section summarizes the statistics for each node or category within the CAISO datasets for 2018-2020, focusing on California. One key aspect of interest is the distribution of energy sources used for power generation in the state.

Table 1.3 highlights the number of observed nodes within the CAISO datasets during this timeframe.

Table 1.3: Summary Statistics of the Nodes

Category	Total Observed Nodes/Hours	Total Unique Power Plant	% of Total Nodes
Natural Gas	7,074,829	282	26.71%
Sun	6,465,547	265	24.41%
Water	6,097,645	208	23.02%
Biogas/Biomass	2,769,718	105	10.46%
Wind	3,058,469	83	11.55%
Geothermal	698,949	26	2.64%
Coal	224,405	6	0.85%
Uranium	100,056	4	0.38%

Source: Author's Calculation

Analyzing the percentages associated with each energy source reveals valuable insights specific to California. Natural Gas is the most prevalent energy source, accounting for 26.71% of the total nodes. This high percentage can be attributed to several factors. Firstly, Natural Gas is a relatively affordable and abundant fossil fuel, making it a popular choice for power generation. Additionally, Natural Gas power plants offer flexibility in ramping up and down their generation capacity, making them well-suited for meeting fluctuating energy demands. The environmental impact of Natural Gas compared to other fossil fuels is also relatively lower, contributing to its widespread usage in California.

Renewable energy sources have also gained significant prominence in California, with sun (24.41%) and water (23.02%) accounting for substantial nodes. These percentages highlight the state's increasing adoption of solar and hydroelectric power. Solar power has grown considerably due to technological advancements, decreasing costs, and favorable environmental characteristics. Water-based energy generation, often through hydroelectric power, has long been utilized in California due to its reliability and relatively low carbon footprint.

Wind power represents 11.55% of the nodes in California, reflecting its significant contribution to the state's renewable energy mix. Wind turbines have become increasingly efficient and cost-effective, making wind power an attractive option for sustainable electricity generation. Additionally, California's favorable wind conditions in certain regions have facilitated the growth of wind energy projects.

The remaining energy sources in California nodes include biogas/biomass (10.46%), geothermal (2.64%), coal (0.85%), and uranium (0.38%). These percentages indicate varying degrees of utilization within the state. biogas/biomass and geothermal energy sources are considered more environmentally friendly than coal, aligning with California's commitment to cleaner energy alternatives. The minimal presence of coal and Uranium suggests a limited role for these energy sources in California, possibly influenced by regulatory constraints, public perception, and the focus on reducing greenhouse gas emissions.

Overall, the observed percentages provide insights into the energy mix within the California nodes of the CAISO datasets. They highlight the dominance of Natural Gas, the increasing adoption of renewable energy sources like sun, water, and wind, and the relatively limited utilization of coal and nuclear power. These percentages align with California's efforts to transition towards cleaner and more sustainable energy generation methods to mitigate climate change and reduce dependence on fossil fuels.

1.3.2 Summary of the *n*-th cheapest hours

Calculating the average n-cheapest Locational Marginal Prices (LMPs) of the day involves sorting the LMPs in ascending order for all months and years of observation.

That allows for identifying the hours with the lowest LMPs on average over the entire period.

For example, determining the cheapest 1-hour LMP for solar refers to the average LMP during the specific day hour when solar nodes have the lowest LMP on average across the entire observation period. Similarly, the cheapest 2 hours LMP represents the average LMP for the two hours of the day with the lowest LMPs, specifically the hours that rank as the 1st and 2nd cheapest on average.

The percentile values associated with these calculations provide additional insights into the distribution of LMPs across the observed hours. Percentiles represent the percentage of values below a certain threshold within a dataset. In this analysis, the percentiles help understand the relative position of the n-cheapest hours to the overall distribution of LMPs.

By examining the average LMPs for different hours of the day, this analysis allows for the evaluation of the cost of electricity during specific periods. This information is particularly relevant when considering the profitability of Bitcoin mining operations utilizing renewable energy sources such as wind, solar, and natural gas.

The resulting data will be further refined within the node/generator, whether there is a negative or non-positive LMP, indicating the power's oversupply in the early hours, such as the first two hours of the day. I will compare the 5th, 25th, 50th, 75th, and 95th percentile of the cheapest two hours of the day. There might be a variation in the negative prices during the early hours of power generation. The summary for the k-th percentile for all the observed resources can be shown in Table 1.4 below.

Table 1.4 shows that the 5th percentile of average cheapest $n = 1, 2, 4$, and 8 hours of the day of all eight primary power sources are negative numbers. Renewables, like wind energy, are the lowest electricity price of all power sources. The sun comes next, although hydropower is the second cheapest electricity price in the lowest n = 2 hours. In this observation, the non-renewables, like natural gas, considered 'clean,' ranked lower

Table 1.4: The *k*-th percentile of average cheapest two, four, and 8 hours by node/category (2018-2020)

Average Cheapest 1 Hour By Node ($/MWh)

category	mean	p5	p25	p50	p75	p95
wind	7.71	-26.44	1.0	15.42	21.62	31.99
sun	8.99	-16.85	1.47	15.1	21.61	32.66
natural gas	11.88	-14.02	4.91	16.46	22.64	33.68
uranium	14.41	-8.3	7.95	16.92	22.65	34.01
biogas/biomass	12.63	-13.48	7.35	17.31	23.32	34.36
coal	12.57	-10.41	5.85	16.23	22.4	33.32
geothermal	11.9	-15.78	6.25	16.46	22.53	32.23
water	9.58	-18.13	5.92	16.97	23.1	33.73

Average Cheapest 2 Hours By Node ($/MWh)

category	mean	p5	p25	p50	p75	p95
wind	9.62	-22.03	3.45	16.13	22.12	32.43
sun	10.87	-14.49	4.31	15.98	22.28	33.31
natural gas	13.74	-10.52	7.9	17.31	23.39	34.47
uranium	15.65	-6.2	10.0	17.65	23.41	34.66
biogas/biomass	14.39	-10.41	9.65	18.04	24.01	35.02
coal	14.28	-8.45	8.37	17.01	23.15	34.2
geothermal	13.45	-13.95	8.32	17.28	23.08	33.03
water	11.92	-15.29	8.36	17.69	23.71	34.5

Average Cheapest 4 Hours By Node ($/MWh)

category	mean	p5	p25	p50	p75	p95
wind	12.36	-16.43	7.38	17.33	23.24	33.97
sun	13.58	-11.34	8.17	17.35	23.53	35.04
natural gas	16.3	-6.64	11.25	18.59	24.71	36.36
uranium	17.64	-3.02	12.28	18.81	25.04	36.47
biogas/biomass	16.87	-6.32	12.26	19.22	25.18	36.64
coal	16.56	-4.81	11.32	18.26	24.45	35.78
geothermal	15.61	-9.8	10.75	18.41	24.13	34.47
water	15.05	-10.24	11.25	18.86	24.8	36.01

Average Cheapest 8 Hours By Node ($/MWh)

category	mean	p5	p25	p50	p75	p95
wind	16.42	-8.95	11.99	19.24	25.24	36.71
sun	17.76	-4.78	12.46	19.57	25.92	38.03
natural gas	19.92	-1.36	14.61	20.7	27.02	39.25
uranium	20.77	0.49	15.18	20.93	27.34	39.6
biogas/biomass	20.3	-1.27	15.23	21.22	27.36	39.42
coal	19.89	-0.48	14.48	20.47	26.7	38.79
geothermal	18.73	-3.33	13.72	20.28	26.09	37.16
water	18.9	-3.68	14.21	20.75	26.84	38.65

Source: Author's Calculation

than coal.[3] Obviously, the longer the hours, such as 4 and 8 hours, the higher the electricity prices, which indicates the more elevated the electricity cost. Also, as the LMPs go from p5 to p25, considerable differences exist in the wind and solar energy categories. The p25 from the average cheapest 2 hours to 4 hours similarly shows the impact of higher electricity prices for the same types (wind and solar) relative to other power sources. However, there are a few differences from the average cheapest 4 hours to 8 hours. The higher percentile

[3]Natural gas is burning natural gas for energy results in fewer emissions of nearly all types of air pollutants and carbon dioxide (CO2) than burning coal or petroleum products to produce an equal amount of energy (eia.gov)

(p50, p75, and p95) presents more positive LMP values with values that do not differ much ($1 - $2 / MWh).

Moreover, comparing the distribution of LMPs for different power sources, specifically wind, solar, and natural gas is valuable. Examining the p5, p10, p90, and p95 values provides insights into the variability of LMPs across these sources.

Figure 1.2 illustrates the distribution of LMPs for each power source from 2018 to 2020, considering all observations. It is important to note that the current presentation combines multiple energy sources, which may lead to confusion. To address this, I will reconsider how to present the data more clearly and effectively.

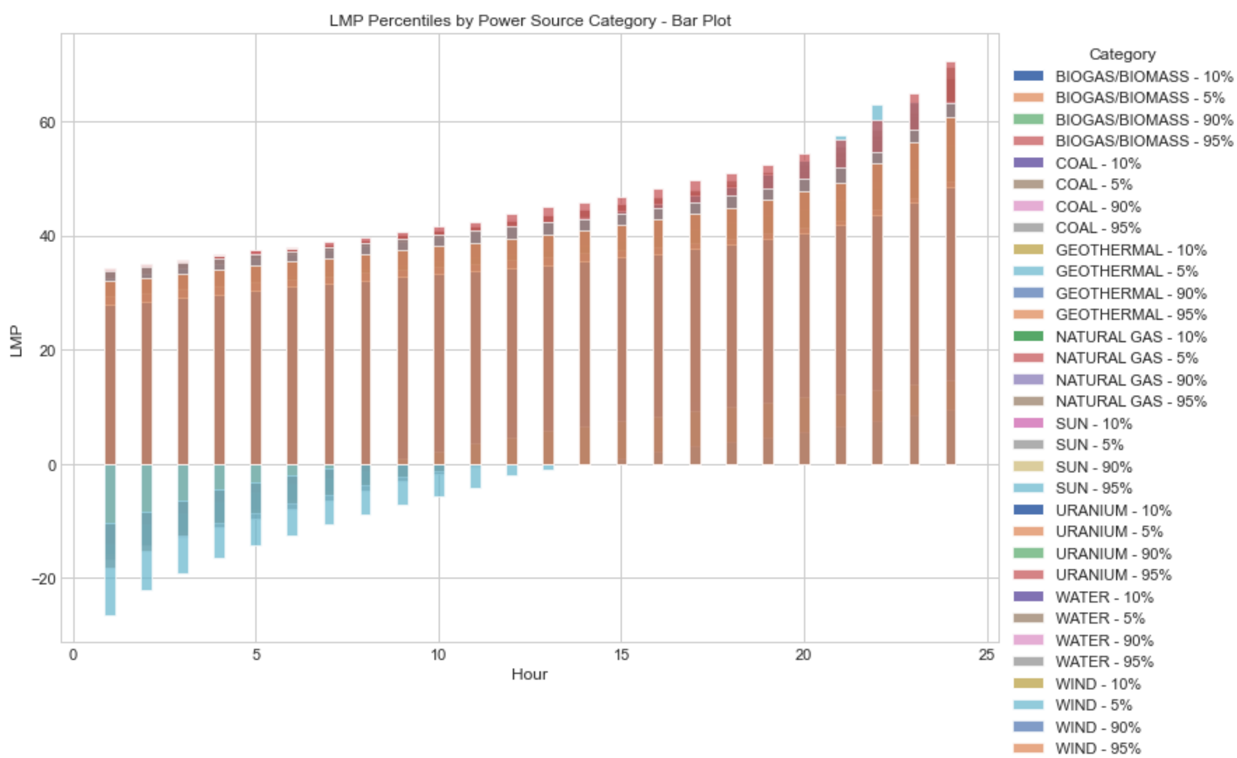

Figure 1.2: 5th, 10th, 90th, 95th Percentile and mean of the average cheapest electricity prices at $n = 1$, ..., 24 hours of the day for 2018 – 2020

Analyzing the p5 for the average cheapest $n = 1,...,24$ hours, I find that wind, solar, water, and geothermal energy consistently exhibit the lowest LMPs. These renewable sources often show negative LMPs from hour 1 (1 am) to hour 13 (1 pm). It indicates that during these hours, electricity generated from renewable sources tends to have lower prices than other power sources. As mentioned earlier, this aligns with the intermittent nature of renewable energy, where its supply comes in spurts.

In contrast, non-renewable sources such as coal, natural gas, uranium, and biogas/biomass generally have average *n*-cheapest hour LMPs around the p90 and p95 values. These sources exhibit positive values for most hours of the day, indicating that their electricity prices are generally higher than those of renewable sources. This observation suggests that mining Bitcoin during the n-cheapest hours using non-renewable sources may not be as cost-effective as utilizing renewable sources during specific periods.

Establishing a clear relationship between the p5-p95 and p10-p90 values is essential. The p5 and p95 percentiles capture the extreme ends of the LMP distribution for each power source, indicating the lowest and highest prices, respectively. On the other hand, the p10 and p90 percentiles provide insights into the LMP range that encompasses the majority of observations for each source. That implies that 80% of the LMPs for a given source fall within the range defined by p10 and p90.

Understanding these percentiles is crucial in comprehending the price dynamics of different power sources throughout the day. By selectively running mining operations during specific hours characterized by lower LMPs, prospective Bitcoin miners can benefit from cost savings, especially when utilizing renewable energy sources that exhibit lower LMPs during particular periods.

To provide a more precise and accurate illustration of the LMP distributions for each power source, I will reconsider the presentation format in future iterations of this analysis. That will allow readers to interpret better and comprehend the variations in LMPs across different energy sources.

Further analysis of LMPs offers valuable insights into the dynamics of electricity pricing within a power grid. In this regard, understanding the distribution of negative LMPs becomes particularly important as it highlights periods and energy sources associated with lower pricing or potential cost-saving opportunities.

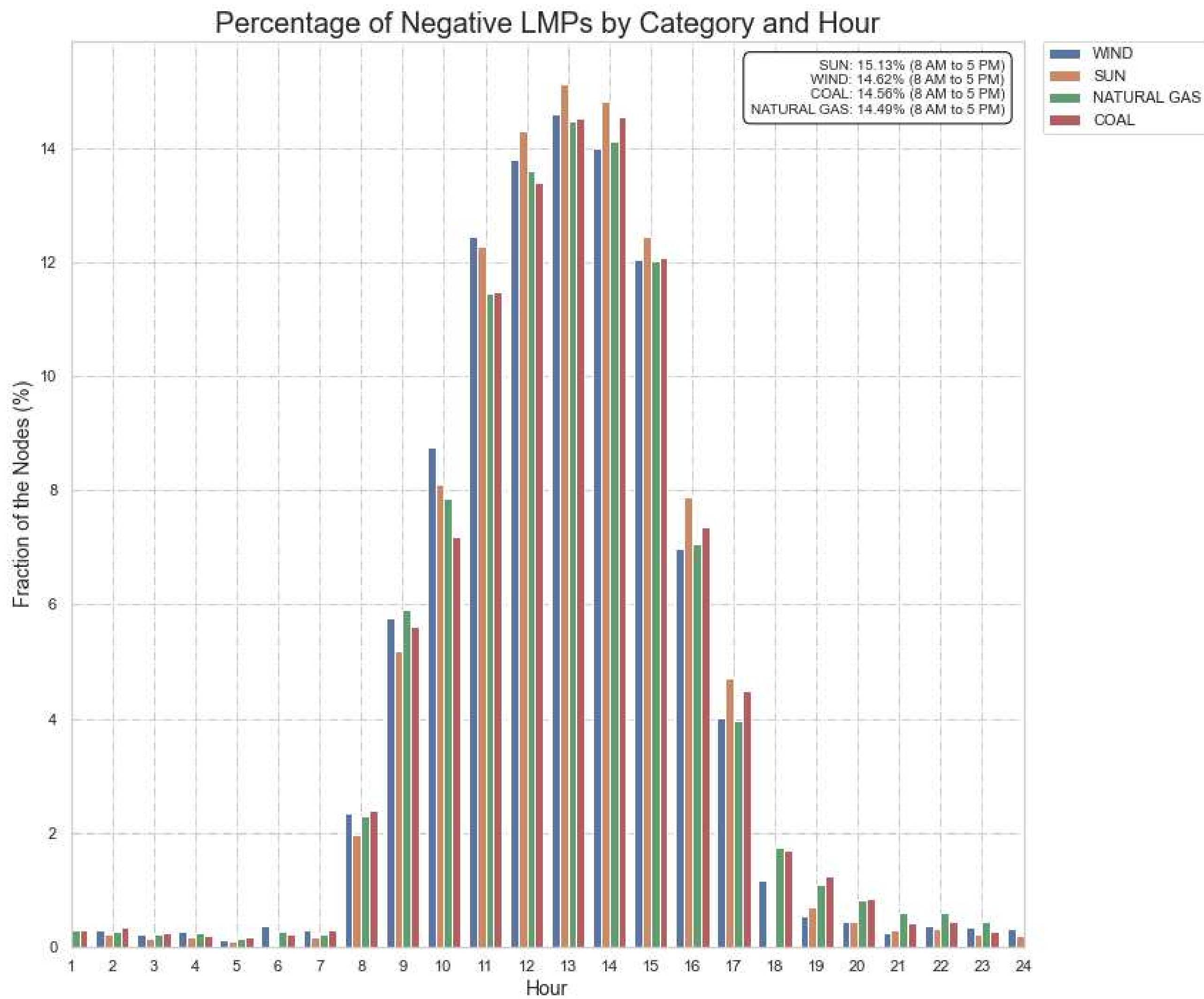

Figure 1.3: Bar Graph for a fraction of nodes at n hours of the day ($n/24$) for 2018-2020 for selected power sources, i.e., wind, solar, coal, and natural gas

Figure 1.3 provides insightful observations regarding the distribution of negative LMPs throughout the 24-hour operation. Notably, hour 13 (1 pm) emerged as a significant timeframe characterized by a concentration of negative LMPs across all selected energy sources. This concentration can be attributed to the dominance of solar energy, which accounted for the highest fraction of nodes experiencing negative LMPs, representing 15.13% of the observations.

Examining the distribution of negative LMPs from 8 am to 5 pm, I observed interesting dynamics among different energy sources. Wind energy claimed the second-highest fraction of negative LMPs, accounting for 14.62% of the nodes, followed closely by coal (14.56%) and natural gas (14.49%). These findings indicate the collective impact of various energy sources on the occurrence of negative LMPs during daytime operations.

Delving deeper into wind energy, I noticed distinct patterns in its distribution of negative LMPs at specific hours. Hours 4 am, 6 am, 7 am, 10 am, 11 am, and 12 am (midnight) I demonstrated a dominant presence of negative LMPs for wind energy. These observations highlight unique factors influencing wind energy pricing dynamics during these hours.

The following section will provide the significance of the colocation for miners to get economic benefits during their 'mining proximity' to the particular power generator location.

1.3.3 Colocation

In this section, I explore the empirical models investigating the possibility of Bitcoin mining. To narrow my analysis, I focus on a specific period of interest in 2019, utilizing preliminary calculations based on Table 1.4. This period reveals a significant disparity in Locational Marginal Prices (LMPs) among wind generators, solar power, and natural gas sources. I aim to identify potential colocation opportunities within this range by examining the average cheapest hours of wind energy generation.

To initiate my analysis, I collect samples for wind power plants with average durations of 1 and 2 hours, as computed in the previous section. By sorting the datasets from the lowest to the highest LMP values, I identify 23 precise plant locations for further investigation. Table 1.5 presents the sorted list of power plant names, providing insights into their respective LMP rankings.

Table 1.5: The average negative LMPs (in $/MWh) of 1 and 2 hours Colocating near the Wind Facilities in California, 2019

Average Cheapest 1 Hour Co-Location

plant_name	LMP
San Gorgonio Farms Wind Farm	-21.56
Painted Hills Wind Park	-21.55
Karen Avenue Wind Farm	-21.55
Mountain View I&2	-21.54
Mojave 18	-21.54
Mountain View IV	-21.54
Garnet Wind Energy Center	-21.53
San Gorgonio Westwinds II LLC	-21.53
Cabazon Wind Partners	-21.48
GPS Cabazon Wind LLC	-21.47
Difwind Farms Ltd I	-20.66
Wintec Energy Ltd	-20.66
Edom Hills Project 1 LLC	-20.34
Altech III	-19.79
Difwind Farms Ltd V	-19.79
Green Power I	-19.79
East Winds Project	-19.79
Dutch Wind Energy	-19.79
Difwind Farms Ltd VI	-19.79
Windpark Unlimited 1	-19.79
Mesa Wind Power Corp	-13.47
Ridgetop	-2.66
Difwind Farms Ltd II	-1.48

Average Cheapest 2 Hour Co-Location

plant_name	LMP
San Gorgonio Farms Wind Farm	-16.03
Painted Hills Wind Park	-16.02
Karen Avenue Wind Farm	-16.02
Mountain View I&2	-16.01
Mojave 18	-16.01
Mountain View IV	-16.01
Garnet Wind Energy Center	-16.0
San Gorgonio Westwinds II LLC	-16.0
Cabazon Wind Partners	-15.95
GPS Cabazon Wind LLC	-15.94
Difwind Farms Ltd I	-15.25
Wintec Energy Ltd	-15.25
Edom Hills Project 1 LLC	-14.93
Difwind Farms Ltd VI	-14.51
Dutch Wind Energy	-14.51
East Winds Project	-14.51
Green Power I	-14.51
Altech III	-14.51
Difwind Farms Ltd V	-14.51
Windpark Unlimited 1	-14.51
Mesa Wind Power Corp	-8.94

Source: Author's Calculation

Shifting my focus to Table 1.6, I find a comprehensive summary of California's top 5 wind power plants based on my prior refinement process. These plants are characterized by their capacity, city/town location, and official names. While Bitcoin mining activities are limited within these wind generator facilities, it is noteworthy that in 2019, Plouton Mining[4] secured $1 million in funding for a proposed sustainable, solar-powered Bitcoin mining complex in California.

Table 1.6: Summary of top 5 wind power plants with negative LMPs in California, 2019

No.	Official Plant Name	Capacity	City/Town
1	San Gorgonio Farms	28 MW	San Gorgonio Pass
2	Painted Hills Repower	39 MW	Riverside
3	Karen Avenue (San Gorgonio Farms)	3 MW	San Gorgonio Pass
4	Mountain View Power Partners II	22.2 MW	Riverside
5	Mojave 16-17-18	84.75 MW	Kern

Source: Author's Calculation

Having explored the specific wind power plant locations and their associated LMPs, I now transition to the subsequent section. I will analyze empirical modeling techniques to investigate the feasibility and underlying factors influencing Bitcoin mining in the following part. I aim to uncover key variables contributing to successful Bitcoin mining operations through regression analysis and hypothesis testing.

1.4 Empirical models of the possibility Of Bitcoin mining

In this section, I will explore empirical models to examine the possibility of Bitcoin mining and its underlying factors. Through regression analysis and hypothesis testing, I aim to uncover the relationships between key variables and the feasibility of Bitcoin mining. By employing statistical techniques, I can gain valuable insights into the factors

[4]See https://cryptoslate.com/mojave-desert-fertile-ground-america-largest-solar-bitcoin-mining-farm/

that contribute to the likelihood of successful Bitcoin mining operations. This analysis provides a foundation for understanding the practical aspects of Bitcoin mining and its associated variables.

1.4.1 Hypothesis

This section is dedicated to examining the impact of renewable energy generation on Locational Marginal Prices (LMPs) through hypothesis testing. Renewable energy sources, including solar, wind, and hydropower, are pivotal in transitioning to a cleaner and more sustainable energy system. However, the intermittency inherent in renewable generation and the presence of bitcoin mining facilities near renewable installations present unique challenges to electricity market pricing dynamics. In this context, this analysis investigates whether renewable energy sources exhibit significantly different LMPs than non-renewable sources.

The hypothesis is formulated for hypothesis testing to accomplish this goal:

H0: *There is no significant difference in the average Locational Marginal Prices (LMPs) per hour between renewable and non-renewable energy sources in California.*

Ha: *The average LMPs per hour are systematically lower in the vicinity of renewables compared to non-renewable energy sources in California.*

The null hypothesis (*H0*) posits no substantial variation in the average LMPs per hour between renewable and non-renewable energy sources in California. That implies that the presence of renewable energy sources does not significantly impact the pricing dynamics of LMPs compared to non-renewable sources within the California energy market.

On the other hand, the alternative hypothesis (*Ha*) suggests that the average LMPs per hour are systematically lower in the vicinity of renewables compared to non-renewable energy sources in California. If the data support the alternative hypothesis, it would indicate that integrating renewable energy sources in California contributes to lower electricity prices, specifically to LMPs, compared to non-renewable sources.

By conducting rigorous empirical analysis to test these hypotheses using California Independent Service Operator data, this study aims to provide evidence regarding the relationship between renewable and non-renewable energy sources and their impact on LMPs in California. The results will offer valuable insights to policymakers, market participants, and stakeholders in shaping energy policies and making investment decisions within the California energy market.

Understanding whether LMPs are systematically lower in the vicinity of renewables in California is crucial for evaluating the economic viability and advantages of renewable energy integration and promoting a sustainable and environmentally friendly energy transition in the state. By examining the pricing dynamics of renewable and non-renewable sources, specifically in the context of California, this study aims to contribute to the knowledge base necessary for informed decision-making and effective energy planning in the state's evolving energy landscape.

1.4.2 Econometrics analysis and results

This section investigates the hourly effect on the Locational Marginal Price (LMP) through econometric analysis. By analyzing the CAISO datasets, I aim to understand the dynamics of electricity pricing and the influence of different power sources across various hours of the day. The LMP is a crucial indicator of the economic value of electricity at specific locations and plays a significant role in shaping energy market outcomes. Understanding the hourly variations in LMPs is essential for assessing the impact of renewable energy integration, addressing intermittency issues, and exploring the possibilities of collocating bitcoin mining facilities near renewable generation sites.

The strategy for the econometrics model employed in this analysis builds upon the extension of Panhans et al. (2017), which explores the effects of variations in electricity costs on environmental policy choices. I will leverage this framework to examine how power sources and their associated costs contribute to LMP fluctuations. Additionally, I will investigate the interaction between hours of operation and the variable of interest for each power source. This approach allows us to assess whether specific hours significantly impact LMPs, providing insights into renewable energy facilities' optimal utilization and collocation.

To accomplish this, I will employ a simple econometrics model that accounts for the 24-hour effect of each power source on the LMP. The model captures the interaction between power source categories, such as biogas/biomass, coal, geothermal, natural gas, sun, uranium, water, and wind, and the corresponding hours of the day. This approach enables us to quantify the hourly variation in LMPs attributable to different power sources, shedding light on the economic implications of renewable energy generation and its integration into the electricity market. The econometrics model is defined as follows:

$$LMP = \sum_{k=1}^{8} \sum_{n=1}^{24} \beta_{kn} \times category_k \times hour_n + \varepsilon \tag{1.1}$$

where,

LMP : Locational Marginal Prices

$hour$: $n \in \{1, \ldots, 24\}$

$category$: Eight power sources of interest:

$k = \{$Wind, Sun, Natural Gas, Uranium, Coal, Biogas/Biomass, Geothermal, Water$\}$

Equation 1.1 represents a multiple regression model that aims to explain the Locational Marginal Prices (LMPs) based on the interaction between different power source categories and the hourly effect. The equation consists of several components:

1. The terms $category_k$ and $hour_n$ denote the categorical variables for a power source category and hourly effect. The equation includes eight power source categories: biogas/biomass, coal, geothermal, natural gas, sun, uranium, water, and wind. Additionally, it considers 24 hours daily to account for the hourly variations in LMPs.

2. The interaction term, $category_k \times hour_n$, captures the combined effect of the power source category and the specific hour on the LMPs. This term allows for analyzing how different power sources and hours influence the prices.

3. Lastly, ε represents the error term, which accounts for unexplained variability in the LMPs that the other variables in the model cannot capture.

By estimating the coefficients $(category_k, hour_n)$ in this econometrics equation, I can assess the impact of power source categories and hourly effects on the LMPs. The coefficients provide insights into how different power sources and hours contribute to price fluctuations and help understand the economic dynamics of renewable and non-renewable energy sources.

1.4.2.1 Hourly effect on LMP

In this section, I delve into the hourly effect on Locational Marginal Prices (LMPs) to uncover the intricate dynamics of electricity pricing across various power sources. My analysis focuses on the variations in LMPs throughout a 24-hour observation period, seeking to unveil patterns and trends illuminating the factors driving pricing fluctuations. To accomplish this, I consider a comprehensive set of power sources, including biogas/biomass, coal, geothermal, natural gas, sun, uranium, water, and wind. By exploring the contributions of these sources to LMPs over specific hours, I can gain valuable insights into the hourly dynamics of electricity pricing.

To understand the hourly effect on Locational Marginal Prices (LMPs), I conducted a detailed analysis in Figure 1.4 visualizing the findings. This will provide a comprehensive overview of the regression results, categorizing power sources into eight distinct categories, offering valuable insights into their specific dynamics, and revealing intriguing patterns in LMP fluctuations throughout the 24-hour observation period.

Figure 1.4 visually illustrates the continuous movement of prices throughout the day, showcasing the interconnectedness of the market and the impact of different power

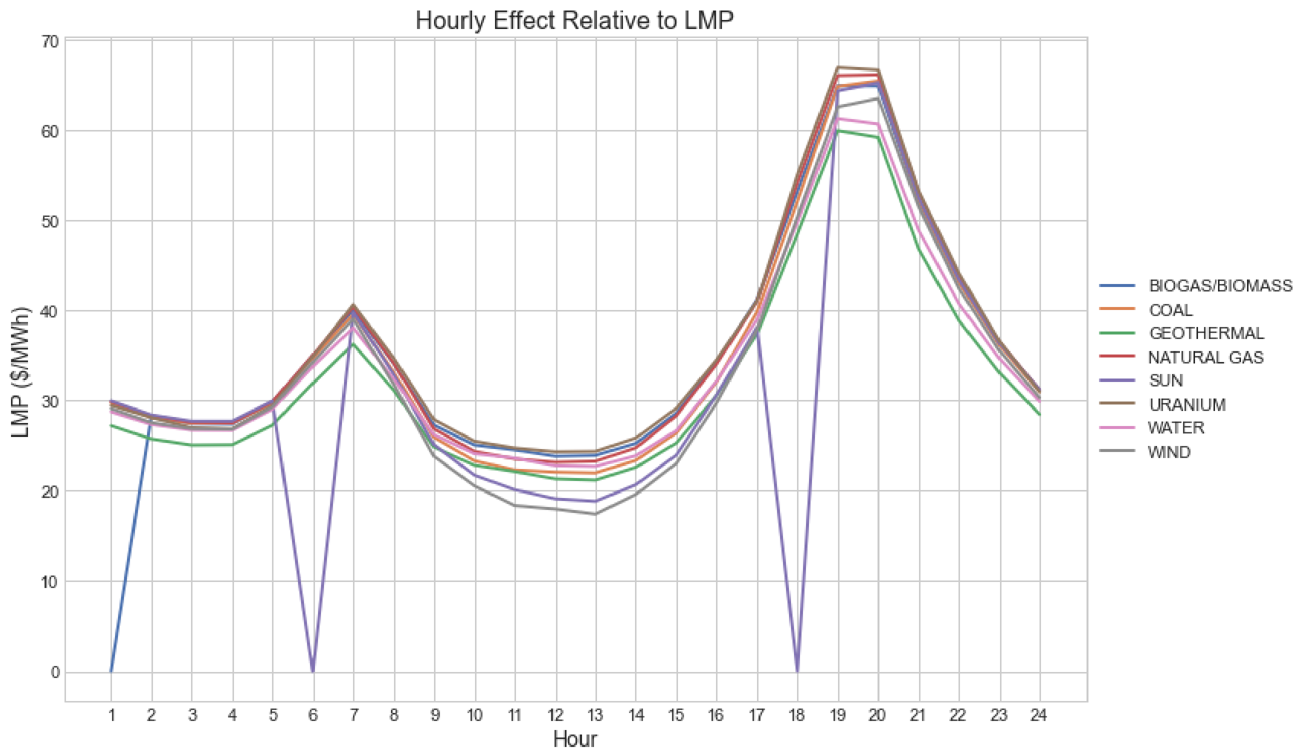

Figure 1.4: The coefficient plots for the eight power sources

sources on LMPs. This visualization effectively represents the dynamic nature of LMPs, highlighting the varying contributions of various power sources.

My analysis indicates that solar power (Sun) consistently exhibits the lowest average LMPs across the observed hours, underscoring its cost-effectiveness. However, it is crucial to note that solar power observations are unavailable for hour 0 (midnight), hour 6 (6 am), and hour 18 (6 pm). This absence stems from the inherent characteristics of solar power generation, as it relies on sunlight for operation, rendering it inactive during nighttime hours. Consequently, I excluded these hours from my analysis.

Further examination of solar power LMPs from hours 7 to 17 reveals that they remain relatively low on average. However, it is worth mentioning that these LMPs are slightly higher compared to wind energy. This finding suggests that while solar power remains cost-effective during these hours, wind energy has the potential to offer even lower LMPs, positioning it as a more economically advantageous renewable energy source within this time frame. The disparity in LMPs between solar and wind energy underscores the significance of considering different renewable energy options and their respective cost profiles to optimize Bitcoin mining operations effectively.

Analyzing the contributions to the lowest LMPs during specific time intervals reveals intriguing patterns. In the early hours (from 1 am to 7 am), Geothermal, Water, and Wind power sources consistently play a significant role in driving down prices. These renewable sources contribute to the lowest LMPs during this period. However, their impact diminishes after hour 15 (3 pm) due to the increasing influence of non-renewable sources during the ramp-up process, signifying a shift in power generation dynamics as the day progresses.

In summary, my analysis highlights the consistent cost-effectiveness of solar power, which exhibits the lowest average LMPs across the observed hours. The exclusion of solar observations during nighttime hours aligns with its dependence on daylight conditions for an effective generation. It focusing the analysis on hours 7 to 17 shows that solar power maintains relatively low average LMPs, albeit slightly higher than wind energy.

The regression results provide valuable insights into the hourly variations in LMPs across different power sources. Solar power maintains the lowest average LMP despite its absence during nighttime hours. Additionally, the contributions of renewables such as geothermal, water, and wind to the lowest LMPs during the early hours highlight the significance of these sustainable sources in the overall energy mix. As I extend the analysis from hour 12 (noon) to hour 15 (3 pm), it becomes essential to consider the changing dynamics of power generation and the increasing role of non-renewable sources during the ramp-up process. These insights can guide strategic decision-making for optimizing Bitcoin mining operations and promote the integration of renewable energy sources to ensure sustainable and cost-effective practices.

In addition to the regression results, the residual plots play a crucial role in assessing the adequacy of the regression model and the normality assumption of residuals, which is essential for reliable statistical inferences. I conducted a regression analysis using the LMP data with category and hour predictor variables to evaluate these aspects, as depicted in Figure 1.5. Each power source displayed distinct characteristics regarding their residuals' kernel density estimation (KDE) and adherence to the normality assumption.

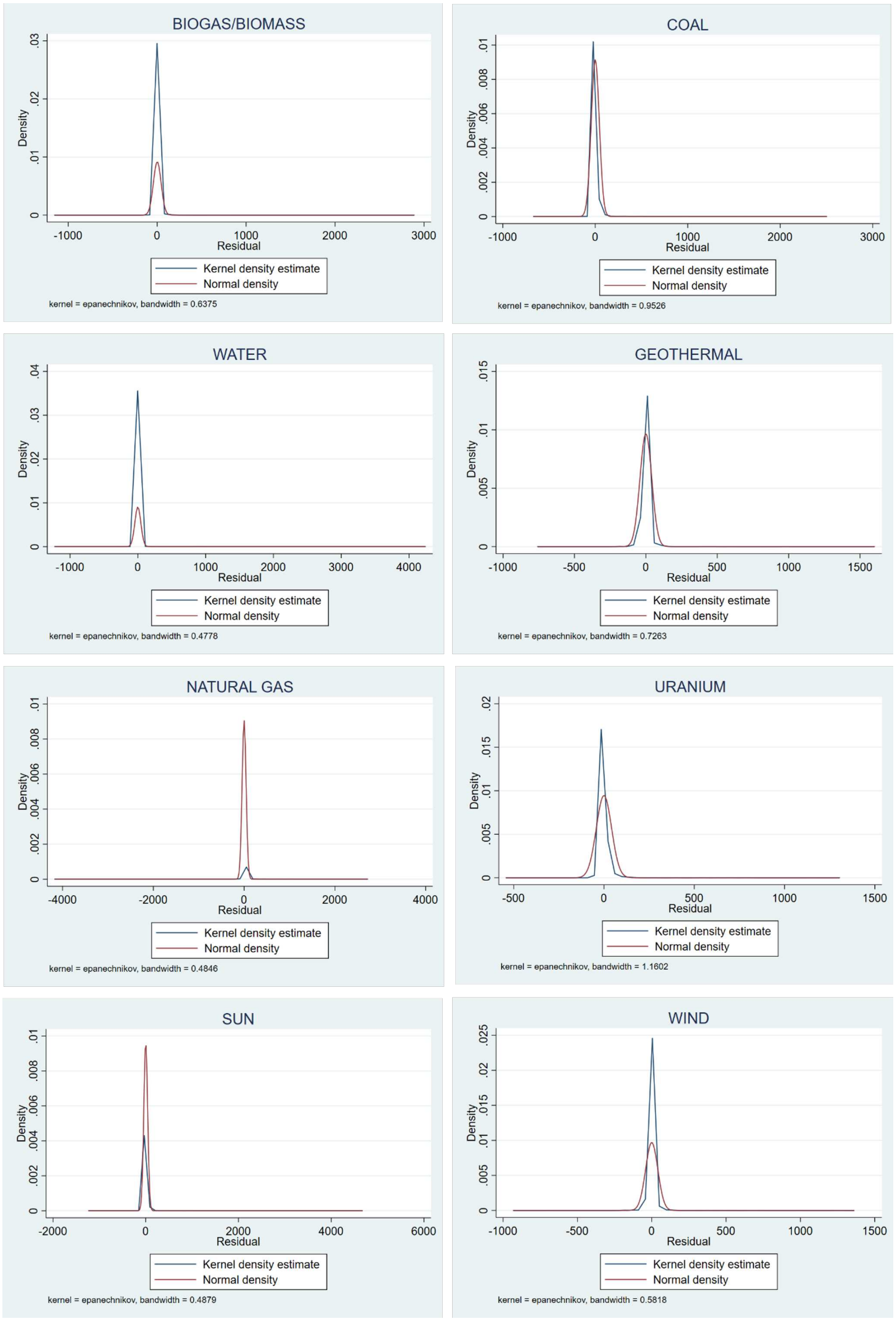

Figure 1.5: Residual plot for all power sources

Biomass/Biogas exhibited a KDE plot with an *epanechnikov* kernel and a bandwidth of 0.6375, showcasing a sharp peak around 0.03 and a relatively flat base without significant skewness. Similarly, Coal demonstrated a KDE plot with a peak around 0.01 and a flat base, suggesting a potential normal distribution. However, Natural Gas showed a slightly left-skewed KDE plot, deviating from the normality assumption. Geothermal displayed a KDE plot with a peak between 0.01 and 0.015 and a minor left skew. Sun and Uranium had KDE plots with sharp peaks around 0.00415 and 0.01505, respectively, while exhibiting slight skewness. Water demonstrated a KDE plot with a peak between 0.03 and 0.04, maintaining a flat base without skewness. Wind showed a KDE plot with a sharp rise at approximately 0.025 and a right skew. These KDE results indicate deviations from the normality assumption for specific power sources, highlighting the importance of considering non-normal residuals in statistical inferences.

Considering the implications for colocation in Bitcoin mining, these KDE findings provide valuable insights into the distributional characteristics of the power sources and their potential suitability for sustainable mining operations. Colocating Bitcoin mining facilities near renewable energy sources, such as wind, sun, geothermal, and water, allows leveraging the lower LMPs associated with these sources. By harnessing the abundant and relatively low-cost renewable energy available during specific hours, Bitcoin miners can potentially reduce their operational expenses and environmental impact.

Moreover, the variations observed in the distributions of renewables and non-renewables have implications for strategic decision-making in Bitcoin mining operations. Analyzing the hourly dynamics of LMPs and understanding the varying contributions of different power sources can inform miners' choices regarding the location and timing of their energy-intensive operations. Collocating near renewable sources during hours when wind, sun, geothermal, and water power dominate the lowest LMPs can lead to significant cost savings and a reduced carbon footprint.

In conclusion, the KDE analysis of the residuals from the regression model provides insights into the distributional characteristics of the power sources. While some sources exhibit KDE plots that align with the normality assumption, others deviate to varying degrees, suggesting potential non-normal distributions. Colocation in Bitcoin mining near renewable energy sources presents cost savings and sustainability opportunities. Miners can optimize their operations and reduce environmental impact by strategically leveraging the hourly dynamics of LMPs and the unique contributions of different power sources. These findings highlight the importance of considering the distributional characteristics of power sources when making decisions in the Bitcoin mining industry.

1.4.2.2 Hypothesis testing: Comparative electricity prices

To rigorously test my hypothesis regarding the electricity prices of renewable energy sources, I perform a *t*-test, a widely used statistical test to assess the significance of mean differences between groups. In this context, the *t*-test allows us to examine whether the mean electricity prices of renewables are significantly lower compared to non-renewable sources. The *t*-test results provide valuable insights into the relationship between renewable energy generation and electricity prices, shedding light on renewables' economic viability and competitiveness in the energy market.

I employ a rigorous methodology that involves statistical analysis. I collect data on electricity prices (LMP) across various energy source categories, including renewables and non-renewables. The dataset comprises observations for each hour of the day (n) and different energy source categories (k). Then, the *t*-test assesses whether there is a statistically significant difference in the mean electricity prices between renewables and non-renewables. The LMP variable is the outcome variable, while the "renewables dummy" variable functions as the grouping variable. Group *Fossil* corresponds to the mean LMP when the "renewables dummy" variable equals 0. In other words, Group *Fossil* represents the average LMP during periods with no or negligible renewable energy generation. That can include times when traditional non-renewable sources such as coal, natural gas, or nuclear power dominate the electricity supply. The mean LMP for Group *Fossil* is 35.5134, with a standard error of 0.0168. This group is a reference point for comparing the LMPs in the presence of renewable energy generation.

Group *Renewables* corresponds to the mean LMP when the "renewables dummy" variable equals 1. Group *Renewables* represents the average LMP when significant renewable energy generation contributes to the electricity supply. Renewable energy sources, such as wind, solar, geothermal, and hydroelectric power, are likely to be the primary drivers in this group. The mean LMP for Group*Renewables* is 33.5790, with a standard error of 0.010. Group *Renewables* allows for examining LMPs, specifically during substantial renewable energy generation periods.

Based on the t-test results in Table 1.7, I observe a significant difference between the mean electricity prices of renewables and non-renewables. Specifically, renewables exhibit prices of 1.9344 units lower than non-renewables, with a standard error of 0.019. The high t-value of 100.1711 indicates a robust statistical significance, supporting my alternative hypothesis that renewables have lower electricity prices than non-renewables.

These findings have important implications for both the energy sector and the environment. The lower electricity prices associated with renewables support renewable energy investments' economic feasibility and attractiveness. Furthermore, the possibility of bitcoin mining near renewable energy facilities leverages the cost advantages of renewables and contributes to the broader goal of sustainable energy practices.

Table 1.7: t-test result

Group	Mean	Std. Error	Std. Dev.	95% CI
Fossil	35.5134	0.0168	45.7125	35.4805 - 35.5463
Renewables	33.5790	0.0101	44.1558	33.5592 - 33.5988
Combined	34.1193	0.0087	44.6045	34.1023 - 34.1363
Diff	1.9344	0.0193	-	1.8966 - 1.973
t-values	100.1711	-	-	-

Source: Author's Calculation

1.5 Conclusion and policy recommendation

The analysis of Locational Marginal Prices (LMPs) reveals promising opportunities for Bitcoin mining through the arbitrage of renewable energy generation. By examining CAISO datasets from 2018-2020, wind and solar power emerge as viable sources for generating profits in the Bitcoin mining industry. The study highlights the average cheapest hours of the day and the fraction of those hours, indicating that lower or negative electricity prices resulting from oversupply incentivize miners to operate during later hours. The variability of negative prices further favors the utilization of renewables over non-renewables like coal or natural gas.

These findings emphasize the potential synergy between renewable energy generation and Bitcoin mining. Collocating mining operations near renewable energy sources, particularly wind and solar power, presents a unique opportunity to capitalize on lower electricity prices. By strategically timing mining activities during periods of oversupply and leveraging the variability of negative prices, miners can optimize profitability and contribute to the sustainable development of the energy sector.

Furthermore, the analysis sheds light on renewable energy sources' economic and environmental advantages. The observed lower or negative electricity prices associated with renewables highlight their competitiveness and economic feasibility. This finding supports the case for increased investments in renewable energy infrastructure, fostering a transition towards a greener and more sustainable energy landscape.

To fully realize the potential of renewable energy-driven Bitcoin mining, policymakers should consider creating a conducive regulatory framework that encourages the development and integration of renewable energy sources. By providing incentives for renewable energy investments, such as tax credits or subsidies, governments can facilitate sustainable energy generation growth and unlock the full potential of this emerging synergy.

However, it is worth noting that this analysis is limited by the absence of power consumption data from CAISO. While this data gap does not directly undermine the accuracy of the regression results, it restricts a comprehensive evaluation of the economics of Bitcoin mining. Future research should focus on incorporating power consumption data from alternative sources, such as the International Energy Agency (IEA) and the US Energy Information Agency (EIA), to provide a more holistic understanding of the energy requirements and potential benefits of Bitcoin mining.

Chapter 2

Assessing the Impact of Bitcoin Prices on Optimal Mining Hours: Implications for Renewable Energy Development

2.1 Introduction

Over the last ten years, Bitcoin has gained popularity as blockchain technology has changed how people transact and connect. In 2008, Satoshi, the pseudonymous founder of Bitcoin, published a vision of a digital currency that, only a decade later, reached a peak market capitalization of over $800 billion (CoinMarketCap, 2018). Cryptocurrencies such as Bitcoin, Ether, Alpha Coin, and Papyrus validate transactions in a decentralized network outside an intermediary, such as a bank for financial transactions or a title company for a real estate transaction.

Most literature reveals that Bitcoin is energy-intensive. For example, Stoll et al. (2019) discovered that the annual electricity consumption of Bitcoin, as of November 2018, was 45.8 TWh. They then calculate Bitcoin's carbon footprint based on its total power consumption and geographic footprint. They found that the annual global carbon emissions of Bitcoin range between 22.0 and 22.9 MtCO2. This ratio sits between the levels produced by Jordan and Sri Lanka and is comparable to the level of Kansas City. Similarly, Jiang et al. (2021) identified that without any policy interventions, the annual energy consumption of the Bitcoin blockchain in China is expected to peak in 2024 at 296.59 TWh and generate 130.50 million metric tons of carbon emission correspondingly.

Even as it consumes abundant electricity, some commentators have gone so far as to claim that Blockchain technology has the potential actually to reduce global carbon emissions. Indeed, Jack Dorsey, former CEO of Twitter, tweeted in 2021 that "Bitcoin incentivizes renewable energy." His other company, Square, teamed up with the firm ARKInvest (which had just bought nearly $20 million of Bitcoin) to author a white paper titled "Bitcoin Is Key to an Abundant, Clean Energy Future." Winton (2021), researcher at ARKInvest, believe that a world with Bitcoin is a world that, at equilibrium, generates more electricity from renewable, carbon-free sources. The idea is that Bitcoin mining can increase the overall share of renewable energy provision to the grid by helping to address the electricity grid storage in a rather unconventional way. In particular, Bitcoin mining can potentially create a productive use for off-peak renewable energy that would otherwise be wasted.

In evaluating this hypothesis, this paper will use historical data on market-based electricity prices in California to empirically test the claim that renewable generators would earn more significant profit by mining Bitcoin during off-peak hours near renewable generators. If so, Bitcoin mining could serve the same role as a "battery" or storage. In particular, by putting the low-value off-peak electricity to productive use, it can potentially make the renewable generator more profitable.

The nature of renewable energy is that its supply is intermittent, meaning that it comes in spurts. For most economic activities, this is a disadvantage but not Bitcoin mining. Because much renewable comes during the day with limited use, the spot price of electricity is low and could be productively used to mine Bitcoin. It refers to the terms of Bitcoin arbitrage. It is the core concept in finance based on the "law of one price," It plays a vital role in financial markets by keeping asset prices in balance with their fundamental values. Arbitrage is the simultaneous purchase and sale of identical or similar financial securities to profit from price discrepancies in different markets (Shynkevich, 2021).

Research questions. The chapter considers the following research questions.

RQ1. Is the opportunity to selectively mine during low-LMP off-peak hours more significant next to renewable generators than it is near fossil generators?

RQ2. How low do Bitcoin prices need to be for miners to optimally choose to mine only a portion of the hours in the day?

To evaluate these questions, I use data from the California Independent System Operator (CAISO) described in paper one, Section 2.2 on the "Empirical Evidence."

I developed a profit-maximizing Bitcoin mining model in this study that incorporates fixed and variable costs. The model considers crucial factors, such as the prevailing Bitcoin price, the quantity of Bitcoin generated, the power consumption associated with the ASIC chips required for competitive mining, and the fixed costs associated with these chips. Specifically, fixed costs, encompassing the initial investment in mining chips, significantly impact overall profitability. By considering these factors, I gain valuable insights into the dynamics of optimal mining hours and the financial feasibility of different mining technologies. Notably, the findings highlight the importance of Bitcoin prices and the need to consider fixed costs in mining operations. With this information, miners can strategically determine the most favorable hours for operation each day while assuming rational expectations regarding Bitcoin prices.

The main takeouts from the analysis are as follows. First, miners will optimally choose to mine Bitcoin during off-peak hours only if the price is less than $3,000. This highlighted result was obtained when considering hourly electricity at the cheapest 5th percentile of wind generators in California during the sample period of 2018-2020. Notably, the threshold price for selective mining to be optimal is far below the average Bitcoin price during this sample period of $8,700. Second, as Bitcoin prices increase, the maximum hours of mining also increase significantly. Third, the break-even prices rapidly decline during the early morning hours, indicating higher cost-effectiveness.

My main conclusion is that the Bitcoin price would have to be much lower than it was during the analysis's historical period for Bitcoin to have the potential to be "green"—lowering carbon emissions despite its voracious appetite for electricity. The study also underscores the significant role of electricity prices in energy economics and their direct impact on Bitcoin mining profitability. It highlights the strategic importance of selective mining during specific hours, considering the efficiency gains achieved through upgrading ASIC technology and the influence of fixed costs. These findings emphasize the dynamic nature of mining profitability, with miners adapting their strategies to optimize returns based on prevailing electricity prices. Understanding these dynamics is essential for miners to make informed decisions and maximize their profitability within the ever-evolving Bitcoin mining landscape.

The paper contributes to several existing literature on Bitcoin mining and economics. First, several previous studies looked at the importance and the economics of Bitcoin mining. For example, Prat and Walter (2021) used the exchange rate of Bitcoin against the U.S. dollar to predict the computing power of Bitcoin's network. They show that free entry places an upper bound on mining revenues and explain how it can be identified. Calibrating the model's parameters allows them to accurately forecast the evolution of the network computing power over time. In practice, operating costs may differ across locations, but miners who have access to the cheapest sources of electricity will find it profitable to enter the market. When hardware becomes more affordable, miners significantly enter the market and devote more resources to electricity consumption.

Similarly, a report by Seel et al. (2021) stated that Bitcoin hashers' preference for renewable energy sources is higher than other electricity uses. The reason is that Bitcoin miners often identify remote, inaccessible locations not connected to the grid. It is common practice to maximize revenue margins. Here, miners can reap the benefits of cheaper renewable electricity produced in surplus and cannot be used and cannot be used, transported, or efficiently stored, for example, surplus hydro, solar, and wind power production.

In comparison, Delgado-Mohatar et al. (2019) estimate that the marginal cost of bitcoin production is around 1,952 US dollars. Below this price, the cost of mining would not be profitable, even with the most efficient equipment and the lowest possible price for the energy required. They have assumed two main kinds of miners, retail and professional, with access to efficiency devices, equipment, and electricity prices. Typically, the first group is located in Europe or the United States and uses commodity mining devices such as the Ant Miner S9, probably the most common device ever used, and consumes electricity at an average price of 0.14 US dollars per kWh. Conversely, professional miners are usually located in China, which has some of the world's cheapest electricity rates. These can be as low as 0.05 US dollars in some regions, such as Sichuan. Current estimates place 70%–80% of global hashing power in China, most of which is in this region. However, through its Central Bank, China's authority has banned the announcement that all transactions of cryptocurrencies are illegal, effectively banning digital tokens such as Bitcoin since 2019 and officially closing the activities in 2021. Hence, this will make the United States the biggest Bitcoin miner since the mining crackdown. The miners have been looking for cheap electricity elsewhere. Significant amounts of mining in the U.S. are based in Washington State, where low-cost electricity from hydropower is available.

The paper will contribute to the existing literature in two ways: (1) The evolution of bitcoin miners' computing power with the advent of the GPU and the dynamics of the electricity prices in the CAISO grid will affect the bitcoin profitability model. The paper will show that different GPU chips would result in different maximum hours so that Bitcoin miners will mine if they find it profitable, i.e., until, for example, more than 24 hours, depending on the ASIC component. The idea is uniquely an alternative to Pratt and Walter's hypothesis that miners' behavior is explained by large variations in the price of their main input producer factor, which is the hardware manufacturers and electricity suppliers; (2) Most economic works of literature discuss the environmental impact of bitcoin mining. For example, Badea and Mungiu-Pupazan (2021) found that the opportunity of evaluating the level of knowledge considering the effects of the Bitcoin mining process on the environment from the perspective of energy consumption and CO2 emissions to finally analyze Bitcoin regulation and identify possible solutions to reduce the negative impact on the environment and beyond. However, only a few papers go into the depth of renewables for charging bitcoin mining, as Jack Dorsey said in his tweets. This paper will argue that renewables will play an essential feature in bitcoin mining and as an opportunity to promote renewable energy such as wind or solar power. The selective mining hypothesis will be a feasible way to explain this concept later in the next section.

The paper is structured as follows. Section 2.2 analyzes the CAISO data to evaluate the variation of Locational Marginal Prices throughout the day, which is the initial step in addressing the first research question. Section 2.3 introduces a theoretical model applied to the data to address the second research question. The quantitative results are presented in Section 2.4, followed by the concluding remarks in Section 2.5.

2.2 Empirical evidence

This section provides an overview of the CAISO data utilized in my analysis. Subsequently, I present the initial set of empirical findings that address the first research question outlined above.

2.2.1 Data

The data on Locational Marginal Prices (LMPs) is the same as that developed in Section 1.3 of the first chapter.

In this section, utilizing the 5^{th} percentile of the average n-cheapest hours of Locational Marginal Prices (LMP) is essential to identify the most cost-effective hours for Bitcoin mining. Opting for the 5^{th} percentile represents a conservative approach to assessing the economic viability of Bitcoin mining operations. Focusing on this lower percentile aims to support the Dorsey hypothesis, which asserts that Bitcoin is environmentally friendly and sustainable. This strategic choice allows for the best chance of reinforcing the hypothesis.

Moreover, this conservative approach aligns intending to showcase findings that prioritize environmentally sustainable practices. By examining the LMP data during these hours, I can determine the optimal time to conduct mining operations, maximizing profitability. Regression plot analysis will be employed to further investigate the relationship between the 5th percentile graph and the profitability model of the selected ASIC chips. This analysis will provide valuable insights into the profitability potential of mining during the identified cost-effective hours, reinforcing the overall focus on conservative and environmentally conscious practices.

In addition to the LMP data, the Bitcoin price is another crucial input for the theoretical model developed in this chapter. To provide context, a historical Bitcoin price plot is included below, allowing us to observe its drastic fluctuations over time. The Bitcoin prices are accessed from *ycharts.com* from 2018 to 2020, which are the value of daily Bitcoin prices. Figure 2.1 shows the historical Bitcoin price value from January 1, 2018, to December 31, 2020. It illustrates the fluctuating bitcoin prices, which peaked after December 2020.

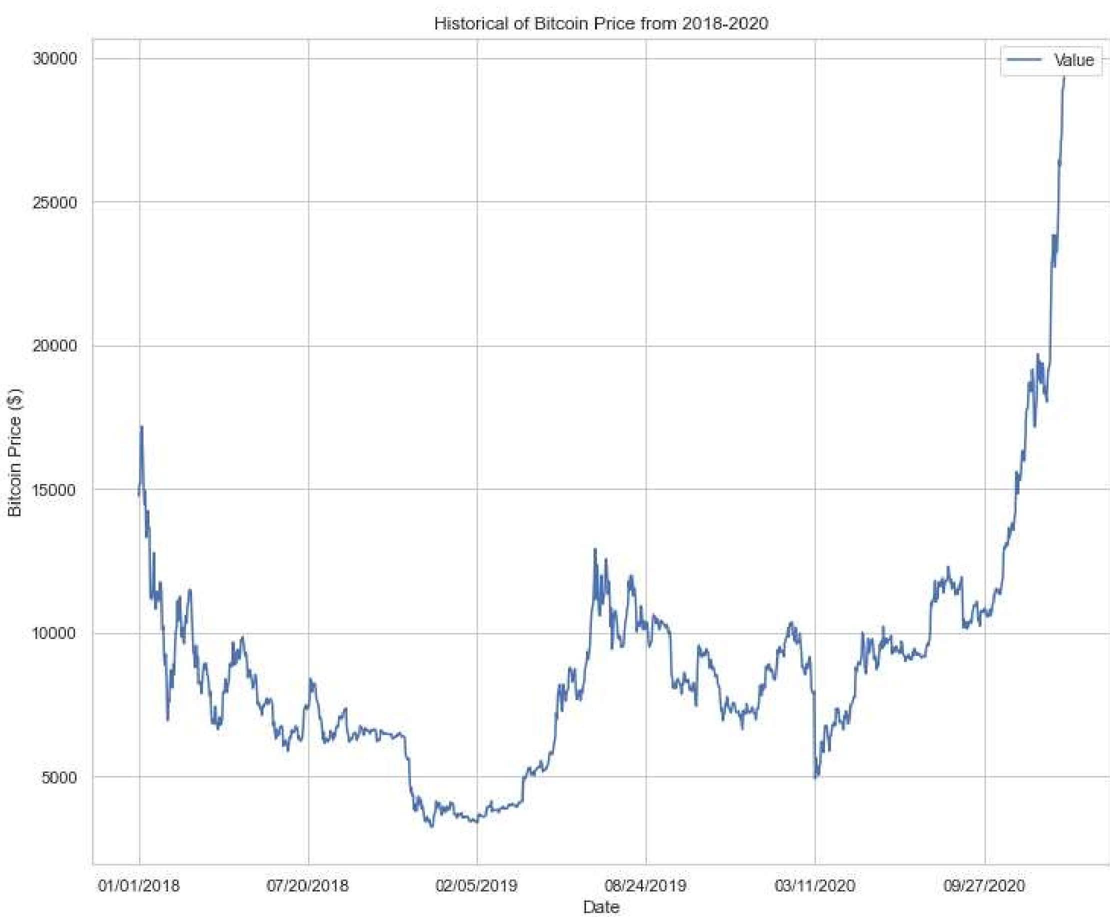

Figure 2.1: Historical of Bitcoin Prices

Application-Specific Integrated Circuits (ASICs), the mining hardware, is aAnother essential part of the equation. It is specialized computer hardware optimized explicitly for Bitcoin mining that is far more efficient for mining Bitcoin than general-purpose computer devices available in typical computers. The data is mainly retrieved from https://www.asicminervalue.com/ for 2017 to 2020. In this research, I take two representative ASICs from the end of 2017, the Bitmain Antminer S9 (13.5Th) and the newer type of the chip, MicroBT Whatsminer M31S+, to compare the effect of the optimal mining hours and the Bitcoin prices.

Finally, Section 2.2.2 incorporates additional data to calibrate and refine the theoretical model, enhancing its accuracy and applicability.

2.2.2 Methodology

Here, I propose a simple methodology to visualize the potential for Bitcoin miners to benefit from selective mining due to historical variation in hourly LMPs across different types of electricity generators. To do this, I use the resource ID variable explained in the last chapter to break the data into three resource types: wind, sun, and natural gas. I calculate the average LMP for each hour of the day for each resource type. I then sort each day into the cheapest to most expensive hours. That allows me to analyze the "n-cheapest hours" averaged across all days in a given year for a given resource type. It is done separately for each year, running from 2018 to 2020. In particular, I calculate the bottom 5% (5th percentile) and the mean of the n-cheapest hours of the corresponding power sources. The n-cheapest hours are computed as follows. For all years (2018-2020) and all day in each hour from $n = 1, \ldots, 24$, I will sort the LMP from the lowest to the highest values and take the average of those values every n hour(s). Then, I will visualize the particular importance of the three power sources. Figure 2.2 shows the average LMPs in ($/MWh) on the y-axis and the related hour (n) on the x-axis. It can be seen that wind power for the whole 24-hour generation is the cheapest of all the observations. Also, it is very interesting to observe the 5th percentile since most negative prices are in that range compared to the mean plot observations.

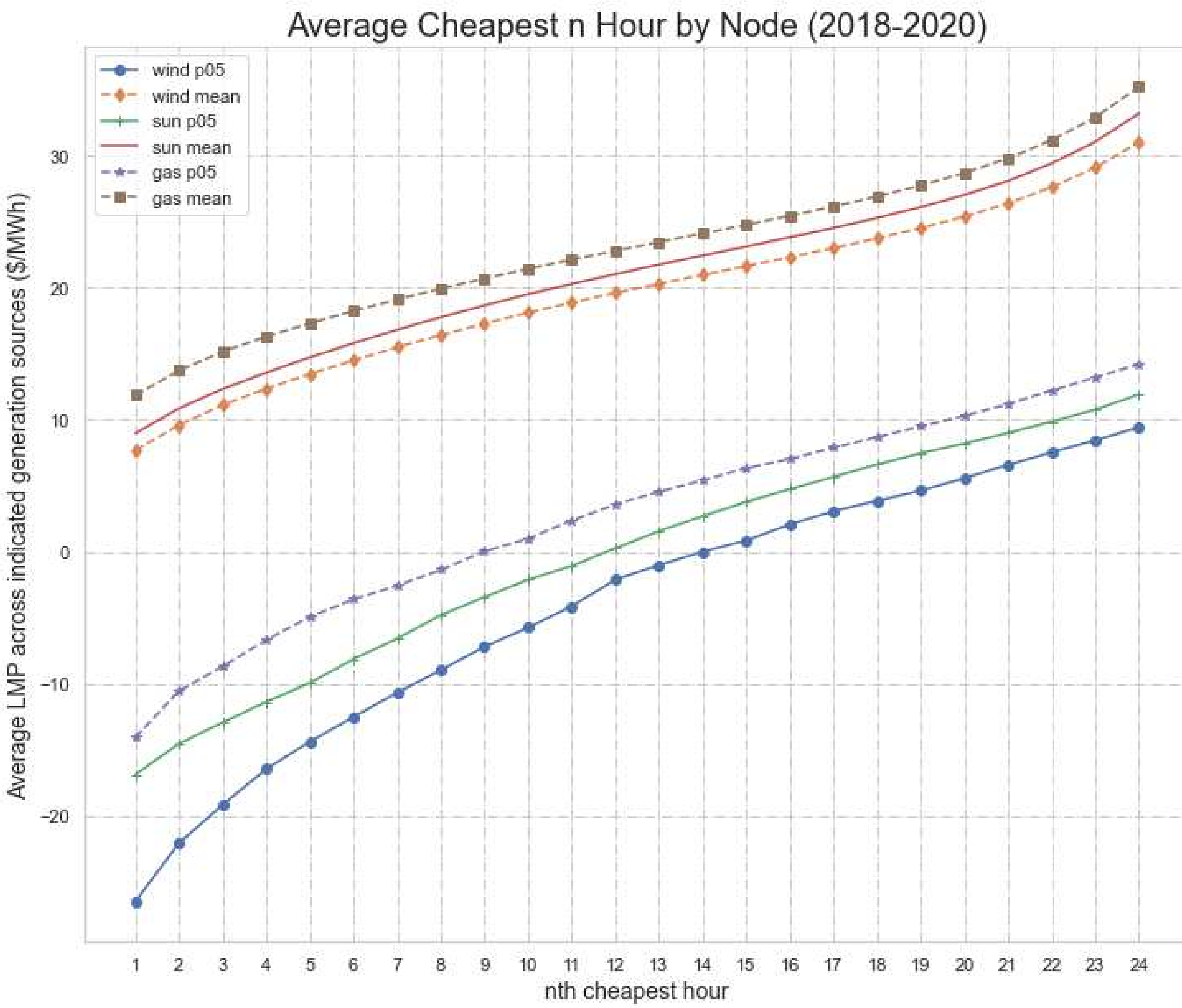

Figure 2.2: The bottom 5% and mean of LMPs for wind, sun, and natural gas technology

The line graph explains explicitly further that each day and each hour, the LMP of the n-cheapest hours for the power sources of interest would be linearly determined by the associated hours of operation for 24 hours.

Furthermore, it is crucial to compare the 5th percentile with the mean or average observation to understand the electricity price dynamics comprehensively. While the 5th percentile represents the lower range of prices, indicating relatively higher costs during those hours, the mean observation provides a broader view of the average price levels. By examining both, I can assess the range and dispersion of prices, allowing for a more comprehensive analysis.

Comparing the 5th percentile and the mean observation, it becomes evident that the 5th percentile tends to exhibit steeper upward curves and more pronounced fluctuations compared to the mean line graph. That indicates that the 5th percentile captures higher price volatility and potentially more extreme price spikes. By focusing on the 5th percentile, I can ensure a conservative approach that considers the potential for higher electricity costs, providing a more realistic assessment of the economic viability of Bitcoin mining operations.

In contrast, the mean observation represents the average price levels across all hours. It provides a benchmark for comparison, offering insights into the general pricing trends and overall electricity costs. The relatively smoother curve of the mean line graph suggests a more stable and predictable price pattern. However, relying solely on the mean observation may overlook specific periods of price spikes or cost-saving opportunities that the 5th percentile captures.

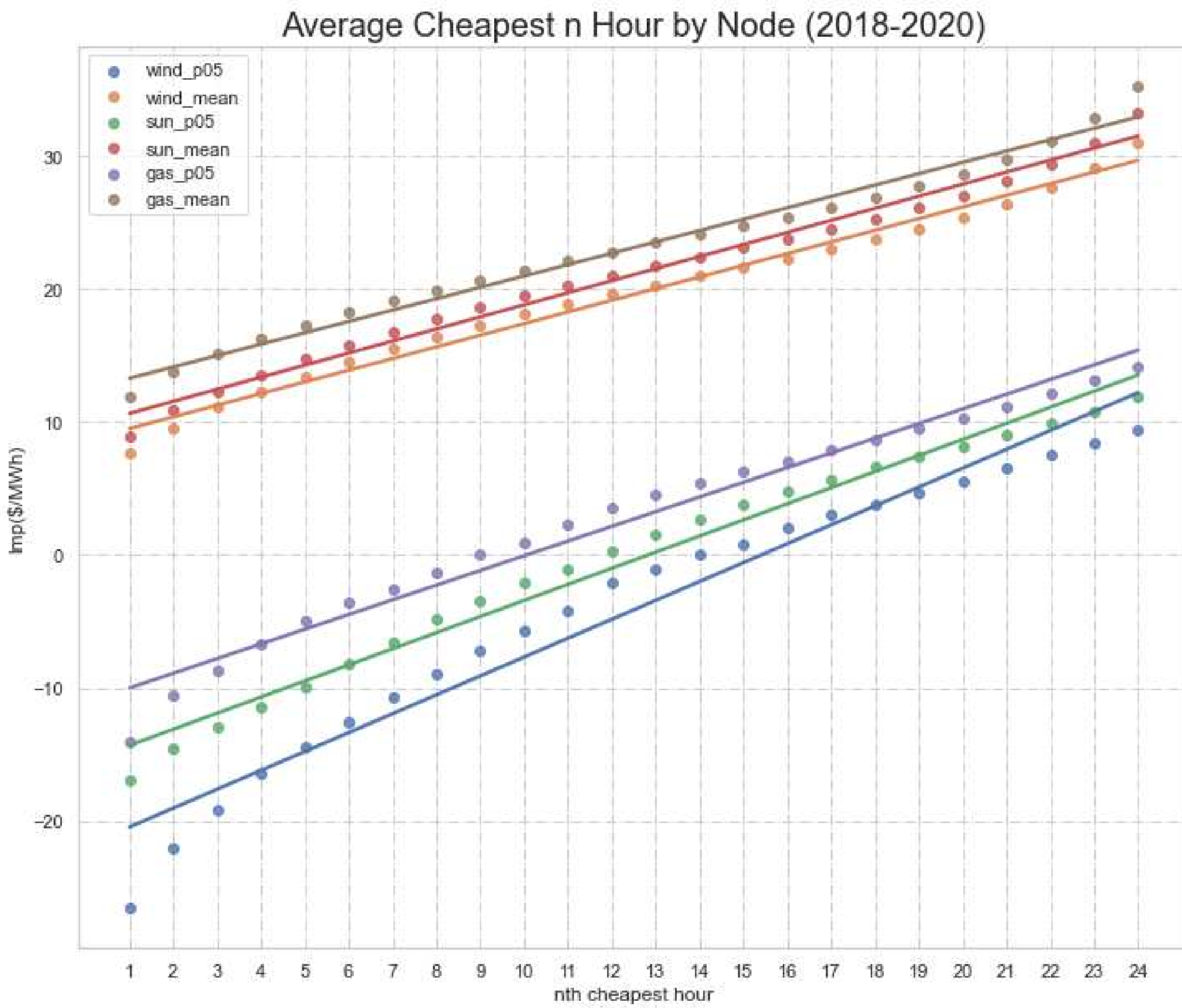

Figure 2.3: The regression plot of the bottom 5% and mean of LMPs for wind, sun, and natural gas technology

Figure 2.3 presents the regression plot derived from the line graph shown in Figure 2.2. The scattered distribution of observed LMP values around the straight-line graph indicates the varying prices associated with each technology. The regression analysis allows us to establish specific equations that describe the relationship between the hour of operation and the corresponding LMP for each technology. These equations form a foundation for modeling the behavior of miners in the subsequent section.

By examining the regression plot, I gain valuable insights into the distinct price patterns exhibited by different power sources. Each technology's equation highlights its unique pricing characteristics, enabling us to understand the cost dynamics and profitability potential during different hours of operation. This information is instrumental in optimizing mining strategies and determining the most favorable timeframes for conducting Bitcoin mining operations.

2.3 Theoretical model

In this section, I will propose a simple model of a profit-maximizing miner to evaluate the incentive to mine selectively during the day. The miner takes as given the relationship between hours of the day mined and the average hourly LMP assuming electricity prices follow the average LMPs shown in Figure 2.3 and assuming the miners have perfect foresight about what electricity prices will be at different times of the day, so they can optimally choose when to mine on a given day. The relationship between the n-cheapest hour and the average LMP is assumed to be linear, as in the fitted model in Figure 2.3. Thus, the miner takes as given the following linear price function:

$$pe^j(n) = a^j + (b^j \cdot n) \tag{2.1}$$

where pe^j is the average n-cheapest hours of LMP for technology j (e.g., wind, solar, and natural gas), a^j is the intercept, b^j is the slope of the equation, and n is the hour from 1 to 24.

The simple profit function:

$$\pi^j(pb, b_n, e^i_n, n, c^i) = (pb \cdot b_n \cdot n) - (pe \cdot e^i_n \cdot n) - c^i \tag{2.2}$$

where π^j is the Profit from technology j (wind, solar, and natural gas) in dollars, pb is the Average of daily bitcoin prices for 3 years (2018-2020) in \$1,000 denomination, b_n is the amount of Bitcoin produced (BTC/hour), e^i_n is the power consumption of particular i ASIC chip in 1 hour (MW), and c^i is the fixed cost of purchasing particular i ASIC chip to run it at the maximum lifetime per hour in dollars.

From Equation 2.1 and 2.2, I can have:

$$\pi^j(pb, b_n, e_n^i, n, a^j, b^j, c^i) = (pb \cdot b_n \cdot n) - ((a^j + (b^j \cdot n)) \cdot e_n^i \cdot n) - c^i \tag{2.3}$$

The break-even price ($\hat{pb}$) is when the profit is zero, meaning that Bitcoin miners would prefer to stop mining when the revenue equals the total costs. So, I can solve $\hat{pb}$ from Equation 2.3:

$$\pi^j(pb, b_n, e_n^i, n, a^j, b^j, c^i) = (pb \cdot b_n \cdot n) - ((a^j + (b^j \cdot n)) \cdot e_n^i \cdot n) - c^i = 0 \tag{2.4}$$

Thus,

$$\hat{pb} = \frac{1}{b_n \cdot n} \left[(a^j + (b^j \cdot n)) \cdot e_n^i \cdot n - c^i \right] \tag{2.5}$$

The profit maximization from Equation 2.3 with respect to n:

$$\frac{\partial \pi^j}{\partial n} = (pb \cdot b_n) - \big((a^j \cdot e_n^i) + (2 \cdot n \cdot b^j \cdot e_n^i) \big) = 0 \tag{2.6}$$

Solve for 2.6, and I get the maximum hour (n^*):

$$n^* = \frac{(pb \cdot b_n) - (a^j \cdot e_n^i)}{2 \cdot e_n^i \cdot b^j} \tag{2.7}$$

Also, to see if Equation 2.3 is the convex or concave function, I can have its second derivative of Equation 2.3 with respect to n:

$$n^* = \frac{(pb \cdot b_n) - (a^j \cdot e_n^i)}{2 \cdot e_n^i \cdot b^j} \tag{2.8}$$

From Equation 2.8, I can see that the curve of the profit function is concave. Thus, it can be expected that there will be a decreasing function of the profit or that there will be maximum or peak points for each particular point.

2.4 Quantitative results

2.4.1 Calibration

In this section, I calibrate the theoretical model above, then show three simulations illustrating the Bitcoin mining profitability model.

The calibration of the parameters is as follows:

1. Parameter pb: average Bitcoin price ($) for 3 years from 2018 to 2020 in a $1000 denomination.

2. Parameter b_n: the amount of Bitcoin (BTC) per hour of observation. How to get the amount of BTC?

   (a) A new block is generated every 10 minutes. There are approximately 6 blocks per hour, 24 hours per day, and 30 days per month, resulting in $6 \times 24 \times 30 = 4,320$ blocks.

   (b) The current block reward is 12.5 BTC/block (until May 2020), so $4,320 \times 12.5 = 54,000$ BTC will be created each month. Antminer S9 (13.5Th) yields a theoretical hash rate of about 13.5 Th/s.

   (c) The current Bitcoin Network Hash Rate[5] is about 51,500,000 Th/s, so Antminer S9 (13.5 Th/s) represents about $13.5/51,500,000 = 0.00000026213592$ of the Bitcoin Network Hash Rate.

[5]Hash rate measures the computational power on a blockchain network. It is determined by how many guesses are made per second. The overall hash rate helps determine a blockchain network's security and mining difficulty

(d) So, the average monthly personal Bitcoin reward for this particular chip is $54,000 \times 0.00000026213592 = 0.01$ BTC. That is $0.01/720 = 0.00001966$ BTC/hour.

3. Parameter c^i: fixed cost for acquiring a particular chip.

4. Parameter e^i_n: power consumption of a particular ASIC chip in one hour (in MW).

5. Parameters a^j and b^j are the intercept and the slope of the average n-cheapest hours of LMP (in a $1000 denomination).

6. Parameter n: hours of the day.

2.4.2 Baseline results

Below, I use MATLAB to solve for and graph the optimal number of mining hours (n^*) for a profit-maximizing Bitcoin miner assuming a range of possible Bitcoin Prices consistent with that observed from 2018 to 2020. The analysis assumes the calibrated parameters as presented in Table 2.1 (For wind p05, solar p05, gas p05) and n = 1, ..., 24 (in hour) and using the Antminer S9 (13.5Th). The results are as follows.

Table 2.1: Calibrated parameters for Antminer S9 (13.5Th)

Parameters	Wind p05	Solar p05	Gas p05
pb_{min} (in $ per BTC)	3.2	3.2	3.2
pb_{max} (in $ per BTC)	29.4	29.4	29.4
pb_{avg} (in $ per BTC)	8.7	8.7	8.7
b_n (in BTC per hour)	0.00001966	0.00001966	0.00001966
e^i_n (in MW)	0.001323	0.001323	0.001323
a^j (in $ per MWh)	-21.8516	-15.5056	-11.0850
b^j (in $ per MWh)	1.4195	1.2103	1.1039
c^i (in $ per MWh)	0.02495	0.02495	0.02495

Source: Author's Calculation
Notes: a^j, b^j, and c^i will be divided by 1,000 to calculate the maximized profit

For different chips, I also use the newer ASICs, MicroBT Whatsminer M31S+, which has a more efficient hash rate (80 Th/s) but a higher fixed or acquiring cost. Table 2.1 comprehensively summarizes the parameters utilized to calculate crucial measures, including the necessary profit, break-even prices, and maximum mining hours. These parameters are derived from Equation 2.4, 2.5, and 2.7 based on the regression plot depicted in Figure 2.3. The values obtained from the regression analysis form the basis for these calculations, enabling us to quantify profitability and assess the feasibility of Bitcoin mining operations during different time periods.

In Table 2.1, the minimum ($pb_{\min}$), maximum ($pb_{\max}$), and the average price of Bitcoin (pb_{avg}) are vital indicators representing the lowest, highest, and average values of daily Bitcoin prices recorded from January 2018 to December 2020. These values serve as reference points for evaluating the profitability of mining operations concerning the fluctuating Bitcoin market.

Additionally, the parameters a^j, b^j, and c^i represent the intercepts, slopes, and fixed costs associated with the respective technologies, namely wind p05, solar p05, and gas p05. These parameters capture each technology's unique characteristics and cost structures, enabling precise calculations of profit margins, break-even prices, and maximum mining hours.

Notably, the negative intercept values in the regression plot's upward slope hold significant implications. They indicate that certain technology deployments can potentially yield negative LMP values, implying the availability of surplus electricity during specific periods. This knowledge is instrumental for miners, as it presents opportunities to mine Bitcoin at minimal or even negative electricity costs, maximizing profitability in favorable market conditions.

2.4.3 Sensitivity analysis

In this section, I consider how the main results vary if I change the energy source from the cheapest wind to other options. This exercise aims to analyze the Bitcoin miners' behavior using the LMPs of three power sources of interest: wind, solar, and natural gas. I also consider the impact of changes in the Bitcoin price.

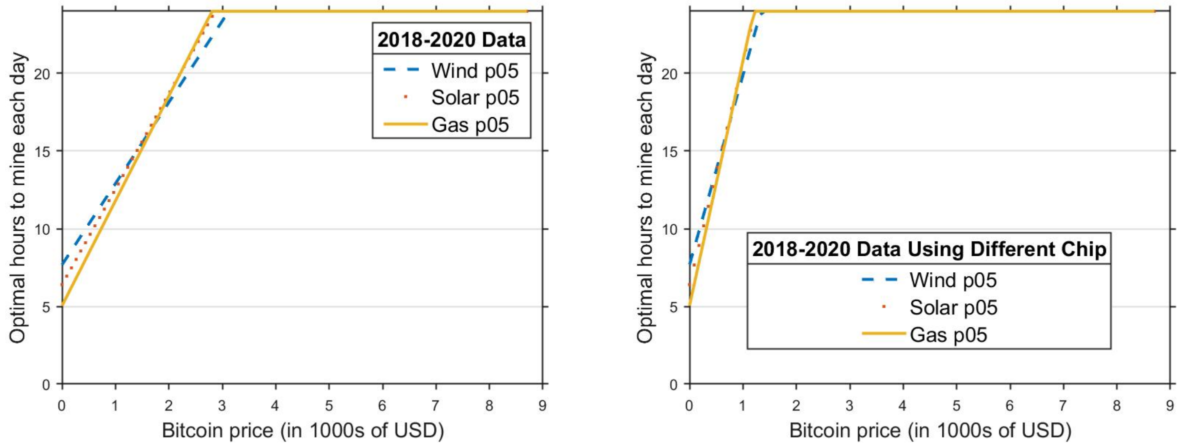

(a) **(b)**

Figure 2.4: Bitcoin prices and the optimal hours to mine each day using ASIC: (a) Antminer S9 (13.5Th), and (b) the newer chip, MicroBT Whatsminer M31S+ (80 Th)

Figures 2.4a and 2.4b visually illustrate the relationship between the optimal hours of mining and the corresponding Bitcoin prices. These graphs provide valuable insights into the dynamics between profitability and Bitcoin market fluctuations. By analyzing these relationships, miners can identify the most reasonable timeframes for conducting mining operations, aligning their activities with periods of higher profitability.

From the above figures, I can conclude that using Wind p05, Solar p05, and Gas p05 technology: (i) in Figure 2.4a, the interesting observation reveals that the overall three technologies coincide at one point, approximately $1,800 of Bitcoin prices and a maximum of hours of 16 (around 4 pm). Further, it shows that for each technology, the miners will selectively choose the Bitcoin Prices ranging from (keeping the positive number) $0 to $3,000 for profitability purposes with more hours on Wind p05 technology. Thus, they should keep mining more than 24 hours beyond that price range; (ii) in Figure 2.4b, the gaps of selective Bitcoin prices between technology are now narrowed (still more mining hours on Wind p05,) and the slope is also steeper than the previous graph, due to more efficient technology with the increasing hash rate; (iii) overall, as the bitcoin prices increase, the maximum hours (n^*) also increases significantly. That means Bitcoin miners will keep mining even for more than 24 hours. The differences in the intercept (a^j) and slope (b^j) values in the electricity price equation, i.e., Equation 2.1, for each energy source (wind, solar, and gas), reflect variations in the cost structure and price dynamics associated with different technologies. However, the analysis in this study focuses on determining the optimal mining hours (n^*) for each energy source rather than directly examining how these differences in a^j and b^j values affect the number of hours miners would use each energy source. Moreover, wind technology provides more maximum hours for bitcoin mining than solar and natural gas technology as the bitcoin prices increase. The bitcoin prices as a proxy to this finding present a critical role for the attractiveness of mining as they provide the sensitivity to the optimal hours of mining, and they will be less responsive as the chip technology improves. Lastly, the hypothesis motivated by Jack Dorsey and Elon Musk that, given the energy prices like wind, solar, and natural gas, would profit-maximizing bitcoin miners optimally choose to mine selectively no longer hold because miners will keep on mining until it is not profitable to do so.

Furthermore, an examination was conducted to determine the break-even point prices ($\hat{pb}$) for various technologies, including wind p05, solar p05, and gas p05, in conjunction with different mining chips. The break-even point price represents the threshold at which Bitcoin miners would consider stopping mining due to the lack of profitability. It is the price at which the total and average profit is zero, indicating that the costs and revenues are in equilibrium. At this point, the marginal profit is also zero, meaning that any further production would not contribute to additional profit.

Figure 2.5 depicts the correlation between break-even Bitcoin prices and mining hours, providing valuable insights that can be analyzed independently. The graph reveals an interesting trend: the break-even prices decrease rapidly from 1 am to 5 am and exhibit a smoother decline afterward. This pattern is observed across all power sources of interest, implying that mining becomes more cost-effective and profitable during these early morning hours.

It is important to note that the cost structure for mining operations must include the one-time purchase cost of the MicroBT Whatsminer M31S+ chip (80 Th), which is 6.65 times that of the Antminer S9 chip (13.5Th). This unavoidable cost significantly impacts the overall profitability analysis and should be accounted for in the calculations. That differs from the profit-maximization approach illustrated in Figure 2.4, where no fixed cost is incorporated into the equation.

By considering these factors, I gain a more comprehensive understanding of the dynamics in determining the optimal mining hours and the financial viability of different mining technologies.

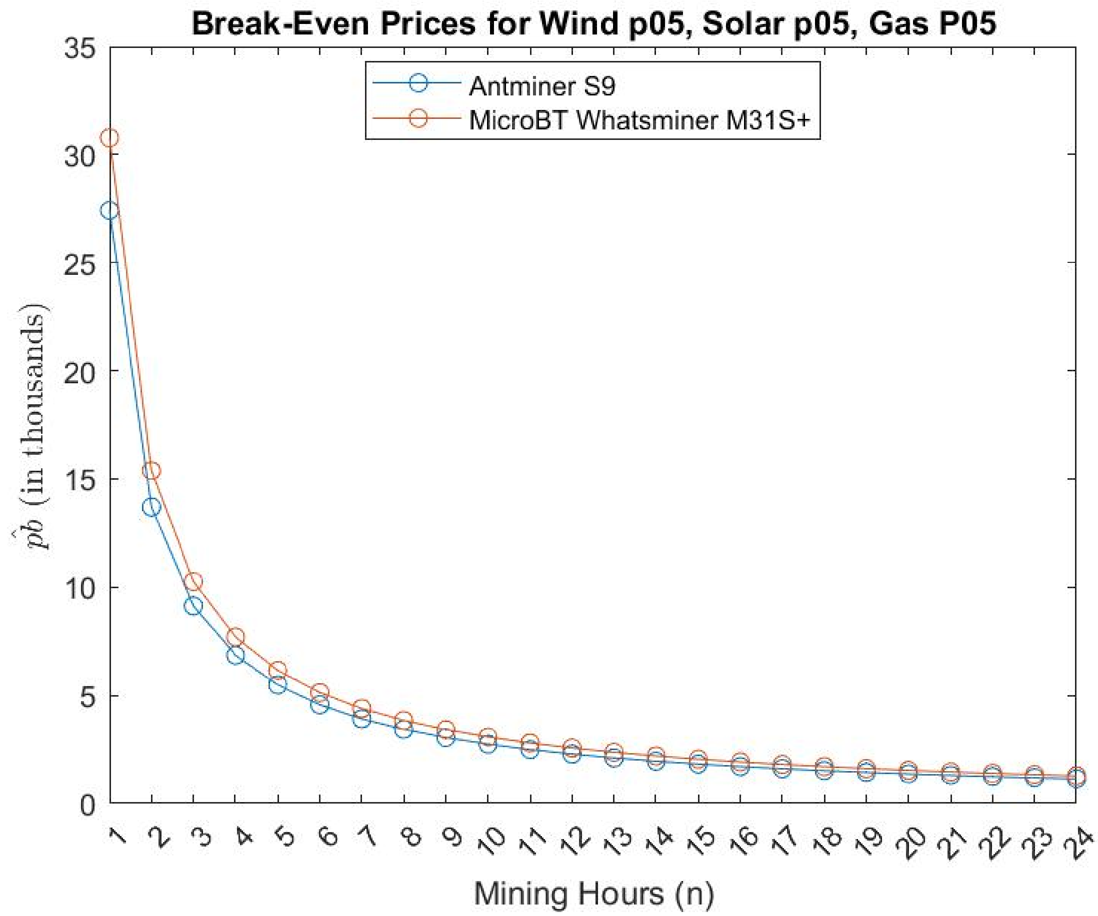

Figure 2.5: Break-even Prices of Bitcoin for each ASIC: Antminer S9 (13.5Th) and the newer chip, MicroBT Whatsminer M31S+ (80 Th) for wind p05, solar p05, and gas p05

The analysis of the maximum achievable profit and corresponding optimal mining hours (n^*) depicted in Figure 2.6a, 2.6b, and 2.6c reinforces the findings observed in Figure 2.4. Across all three power sources, the profit maximization analysis indicates that Bitcoin miners can maximize their profits by mining for more than four hours without imposing restrictions on their mining hours. That suggests miners can extend their operations beyond the initial four-hour threshold to optimize their profitability. It is noteworthy that among the evaluated power sources, wind power emerges as the most profitable option. On the other hand, solar and gas power offer relatively lower profit margins. This finding suggests that miners can optimize their earnings by prioritizing wind power as their preferred energy source for mining operations.

Furthermore, addressing the limitations imposed by solar power's restricted availability is important. Since solar power can only be utilized for a hypothetical maximum of 12.43 hours per day, I have set an upper bound of 12.43 on the x-axis for solar observations. The theoretical model suggests that mining for 24 hours a day would yield the best results, but in practice, it may not be feasible or desirable. Thus, I have included a vertical line to indicate that solar mining operations would cease after 12.43 pm. Additionally, it is important to note that while solar power offers certain limitations due to its reliance on sunlight, wind power provides a reliable alternative by offering a consistent energy source regardless of the time of day or weather conditions. This further underscores the rationale for considering wind power as a viable option for Bitcoin mining operations.

It is also interesting to note that the optimal profit for Wind p05 starts around 7.50 am and continues for 24 hours. In contrast, for Solar p05, the optimal mining hours range from approximately 6.30 am to 12.43 pm. Gas p05, on the other hand, indicates optimal mining hours starting as early as 5 am and continuing for 24 hours. This analysis provides valuable insights for Bitcoin miners, empowering them to make informed decisions regarding their operational strategies and ensuring they capitalize on the most financially profitable opportunities.

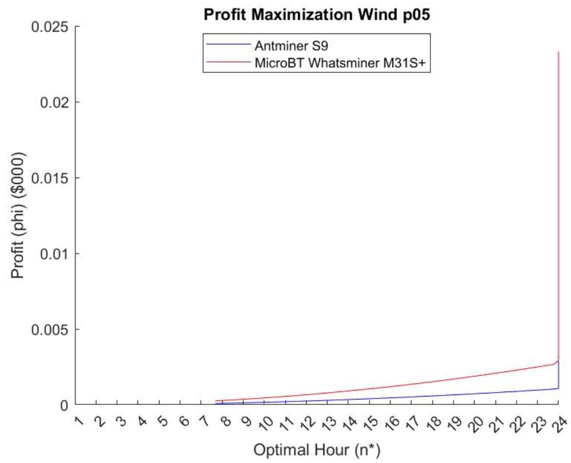

(a)

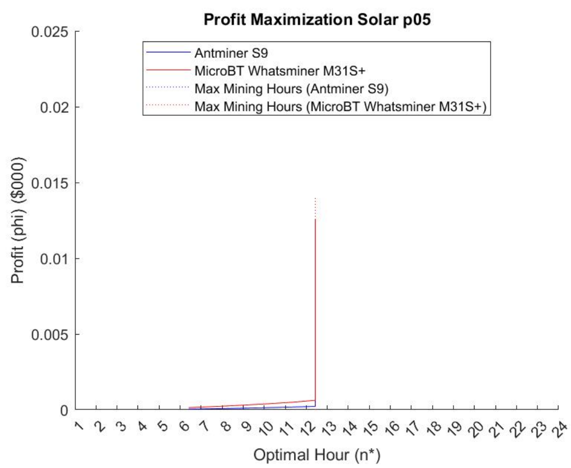

(b)

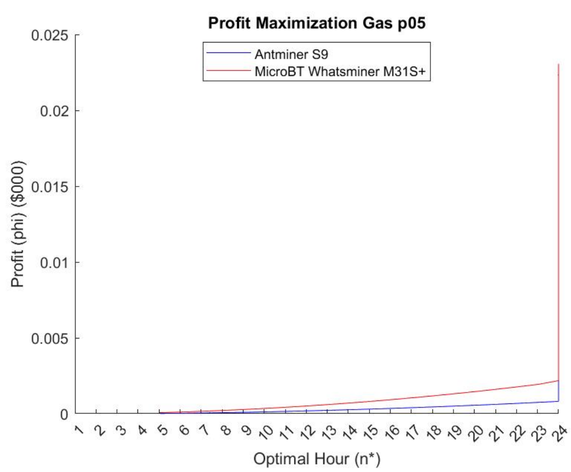

(c)

Figure 2.6: Profit maximization with the optimal hour of different chips using (a) wind p05, (b) solar p05, and (c) Gas p05

There are several limitations to consider in this study. Firstly, it assumes that the observed LMPs from power sources in CAISO are isolated from adjacent grid interconnections within the USA, potentially overlooking trading dynamics and fluctuating electricity prices resulting from interconnections with entities such as ERCOT, Alberta Electric System Operator, or Southwest Power Pool. Secondly, due to time constraints and the complex structure of the CAISO dataset, the study does not consider the load of each power source, which can significantly impact Bitcoin mining operations. Additionally, while the Bitcoin mining market is described as oligopolistic with asymmetric firms, this analysis assumes a free-entry market. It does not directly consider geographical factors influencing mining locations, as Delgado-Mohatar et al. (2019) discussed. It is important to note that most bitcoin mining operations currently colocate near hydropower facilities in China and the United States, as highlighted by Schinckus (2021), Wang et al. (2019), and Johansson and Göransson (2020), due to factors such as affordable electricity costs, surplus power availability, and favorable feed-in tariff rates. However, wind and solar power are still viable options for several reasons. Wind power offers a renewable and abundant energy source, while solar power provides the advantage of scalability and environmentally friendly energy production. By incorporating wind and solar power into the mining operations, miners can diversify their energy inputs, contribute to the development of sustainable practices, and reduce their reliance on a single energy source. Therefore, despite the prevalence of hydropower colocation, wind and solar power present attractive alternatives that align with the goals of renewable energy utilization and support the long-term sustainability of Bitcoin mining operations.

2.5 Concluding remarks

Electricity prices have become the major components for the economics of energy calculation due to their sensitivity to the energy market's short- and long-term demand.

CAISO LMPs datasets provide good critical analysis to observe different technology, like renewables, i.e., wind or solar energy, or natural gas, for an opportunity for Bitcoin mining.

Using quantifying the incentive that Bitcoin miners face to mine selectively during the day would benefit Bitcoin miners in identifying the cheapest ways to maximize their profits. The paper concludes that utilizing them at a particular time is necessary due to the nature of renewables, i.e., intermittency issues where they come during the day with limited use and the variation of the corresponding LMPs (mostly low in values). The sensitivity analysis shows that as the Bitcoin prices increase, miners will undoubtedly keep mining for more than 24 hours a day if the ASIC technology is qualified. Most ASICs nowadays have been improved to run efficiently, gaining a lot of profits for whole days as new components have been invented. The latest ASIC, Bitmain Antminer S9 (13.5Th), has evolved to the new variants, Bitmain Antminer T19 Hydro (145Th), released in October 2022, that has a hash rate of 9.7 times than its predecessors.

Fixed costs, like ASIC mining equipment, will also play an important role in determining how long the mining takes. I find that switching to newer ASIC reduces the level of Bitcoin prices that miners would find lucrative. Garratt and van Oordt (2020) explain that because mining equipment lasts less time, the equilibrium level of mining power corresponding to any fixed cost level must drop to make mining per period more profitable. That means miners have more income per period to lose. Fixed costs gain weight in the miner's decision because they must be earned back quickly, while the present value of the future per-period cost becomes smaller.

The limitation described before in this study will be sorted out as follows: (i) First, this paper will be extended for the possibility of getting the energy loads data from different sources, like Energy Information Administration (EIA), so it will be a lot easier to sort LMPs based on the highest load datasets; (ii) Then, I will modify the model into the real-world problem that incorporates the different geographical locations or bitcoin mining hubs. Lastly, on further research, if time permits, I will look at the government policy, like taxes on the bitcoin mining decision using renewables, as they will contribute to the profitability model I develop in this paper.

Chapter 3

Exploring the Effects of Production Tax Credits on Renewable Energy Development: A Computable General Equilibrium Approach in East Indonesia

3.1 Introduction

As a member of the Paris Agreement, Indonesia shares in the joint goal to ensure that i) emission reduction promises are kept to maintain the global temperature rise to 1.5°C; ii) countries that are vulnerable to climate change that committed to the issues of adaptation, loss, and environmental degradation are respected; iii) mobilize financing for climate change in private and public sector finances needed to secure global net-zero emissions; iv) all countries work together to accelerate action to address the climate change crisis through collaboration between government, private/business, and civil society. To implement this goal, the Indonesian government has formulated a road map to achieve global net-zero emissions by 2060, which is outlined in five central principles/initiatives, a) increasing the use of new and renewable energy (NRE); b) reduction of fossil energy; c) electric vehicles in the transportation sector; d) increasing the use of electricity in households and industry and e) utilization of Carbon Capture and Storage (CCS).

The stated plan is that NRE in Indonesia's energy mix will reach 87% by 2050. Then, in 2060, the NRE portion would reach 100%, with Solar Power Plants and Hydropower being the dominant energy generation sources. The goal is to distribute a gas network of 23 million household connections, 52 million household electric stoves, the use of electric vehicles, and the consumption of electricity that will reach 5,308 kWh/capita.[6]

---

[6]See https://ebtke.esdm.go.id/post/2022/02/21/3091/masa.transisi.energi.menuju.net.zero.emission (in Bahasa Indonesia language)

In early steps toward meetings these ambitious long-term goals, the government of Indonesia has started to pursue projects to begin this transition. For example, through the Ministry of Energy and Mineral Resources (MEMR), the Indonesian government is developing a large-scale hydroelectric power plant with a capacity of 9 GW in North Borneo Province. The project is integrated with developing green industries under the Renewable Energy Based Industry Development (REBID) program. In addition, starting in 2025, a Super Grid[7] will be designed to provide energy access for local communities throughout Indonesia. A Super Grid is a broad area transmission network generally transcontinental or multinational. This network will allow large amounts of electricity to trade across great distances. The enhanced grid capacity will support the national energy transition, allowing increasing amount of intermittent renewable energy to be used.

In the Timor System, Indonesia, as shown in Figure 3.1, specifically in six counties, including Kupang City, Kupang, Timor Tengah Selatan, Timor Tengah Utara, Belu, and Malaka, there is a total area of 5,609.4 square miles and a population of approximately 1,492,385 households. This region is known for its diverse industries, which include salt production, seaweed cultivation, shrimp farming, tuna fishing, and lobster fishing.

There are plans for power plant development to address the energy needs of this region. By the year 2030, a 30 MW Solar Power Plant will be built in Kupang, harnessing the abundant sunlight of the area. Additionally, there are efforts to transition the existing coal power plant into a smaller-scale facility, reflecting the growing emphasis on renewable energy sources.

However, the development of renewable energy in this region faces certain challenges. The primary obstacles include the limited demand for electricity, particularly in the industrial sector, and inadequate infrastructure, including electricity groundwork. Consequently, most renewable energy development in the eastern region is currently focused on small-

[7]See https://www.esdm.go.id/en/media-center/news-archives/energy-minister-spells-out-energy-transition-road-map-in-meeting-with-world-bank

scale projects. There is a need to provide facilities and incentives to industries involved in the renewable energy sector to overcome these infrastructure challenges, particularly in solar and wind energy. These incentives can help alleviate the initial investment burden and facilitate the procurement of raw materials for infrastructure development.

Research questions. Entering the current public policy debate on these issues, this study will attempt to answer the following main research question:

RQ1. What would be the economic impact of imposing a PTC on the NRE industry in Indonesia?

RQ2. In particular: What are the impact on economic activity, the profitability of domestic firms, household consumption and welfare for electricity consumers, and the public tax base in the East Nusa Tenggara (NTT) or Timor System Region? The research will provide the first quantitative assessment of the economy-wide impact of a PTC in Indonesia, providing the first estimate of the multiplier effect of such a tax on economic activities in the Timor System area. The multiplier could eventually be used to help determine the optimal electricity price in subsequent analysis.

This paper has five sections. Section 3.2 describes the theoretical foundation of the economics of the energy transition from fossil fuels to renewables and the Computable General Equilibrium (CGE) model for the energy sector in general with its application. Section 3.3 describes the data collection and analysis that underlie the results. In Section 3.4, I present and interpret the results. Finally, Section 3.5 concludes.

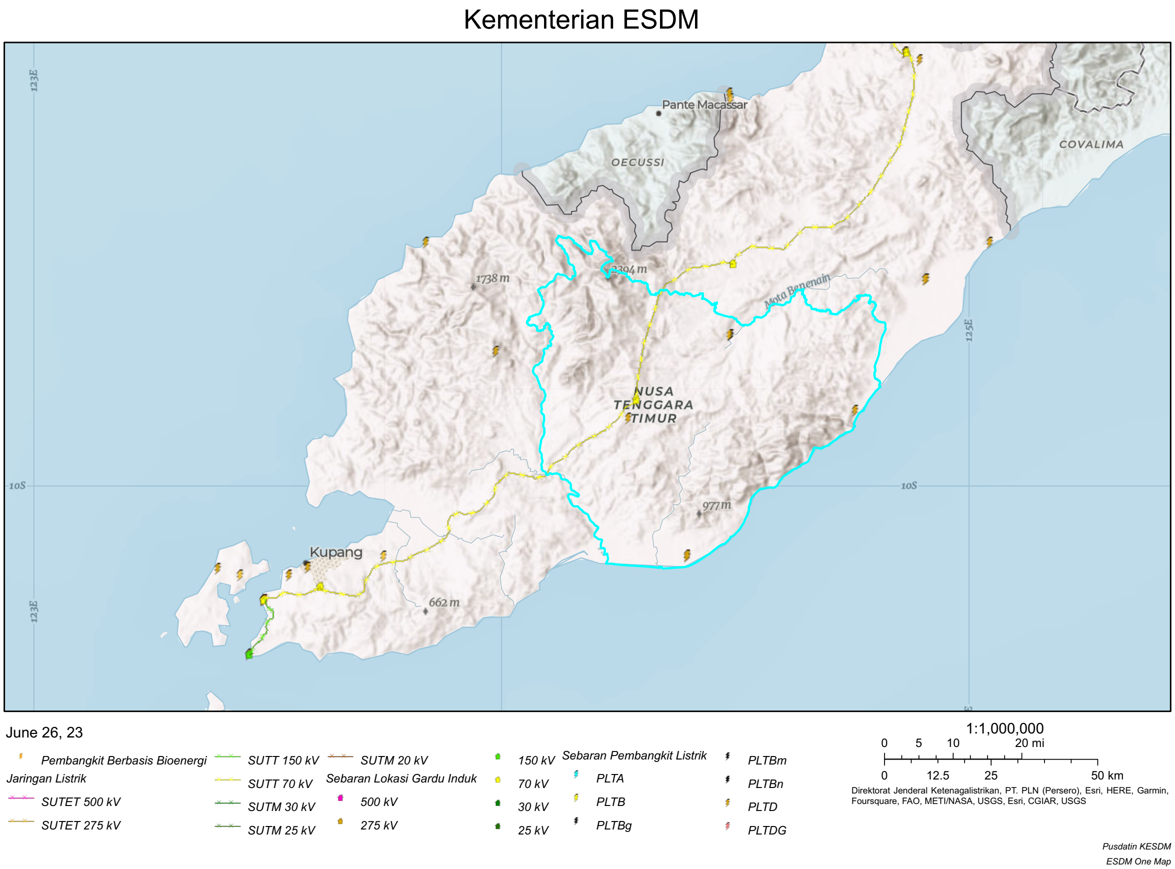

Figure 3.1: Electricity Map of Timor System (Source: Indonesia's Ministry of Energy)

3.2 Previous studies

The paper contributes to several related literature. First, it contributes to a literature that considers energy subsidies in Indonesia. In their study, Isdinarmiati and Oktaviani (2012) concluded that increasing the Basic Electricity Tariff (BET) carried out by the government both in the short and long term hurt Indonesia's macro and sectoral economic performance. On the other hand, in their research, Yusuf and Resosudarmo (2008) used the CGE model with disaggregated Households. The analysis was then used to see the effects of the energy price reform package, the October 2005 Package. They simulated increasing domestic fuel price (kerosene), which increased inequality, especially in urban areas.

Then, there is literature from outside Indonesia which discusses a lot about the topic of energy and environmental economics, including those relating to the effect of clean energy on actors in economic activity in society, namely producers, consumers, and the public sector or government. For example, Hannum et al. (2017) use the CGE model to calculate the number of incentives to support the acceleration of NRE, especially wind energy, in the form of PTC and Renewable Portfolio Standard (RPS).

In addition, Freire-González and Puig-Ventosa (2019) research concludes that the energy transition to clean energy sources will reduce the negative environmental impact. Meanwhile, Oei et al. (2020) stated the importance of combining policies to overcome unemployment and attract NRE companies and investment and measures to improve infrastructure, education, research facilities, and location factors in the development of NRE.

On the other hand, Keyser et al. (2021) mentioned that, in 2019, the City of Los Angeles committed to converting its electricity portfolio to 100% renewable sources by 2045. With this initiative, the substantial changes in transmission and distribution network issues result in essential changes to significant investments in renewable energy generation and changes in operations and maintenance spending. As part of this transition, electricity prices will also change, reflecting the financing of expenditures related to new investments and changes in marginal production costs that arise when switching sources (e.g., coal versus wind). To analyze this issue, they use the CGE models to estimate the economic impacts of the proposed transition under various scenarios relative to a reference case. They use expenditures that are disaggregated into specific energy technologies and estimates of changes in average electricity costs and rates for each scenario. Their primary indicators of interest are total regional gross output (equivalent to domestic supply or sales revenue), total employment, and the level of distribution of real household income.

Other papers explain the particular CGE models for the electricity or energy sectors. For example, Cai et al. (2015) use the Global Trade and Environment Model (GTEM-

C) to model heterogeneous electricity technologies like Coal, Natural Gas, Solar, and Wind. They conclude that the general equilibrium approach reproduces the structure of the global economy and records the economic transactions among regional producers and households. A similar paper, such as McKibbin and Wilcoxen (1999), describes the intertemporal computable general equilibrium (CGE) model of the world economy called G-Cubed to compare a power-sector-only climate policy with economy-wide measures that place the same price on carbon or achieve the same cumulative emissions reduction. They inferred that from the Global Trade Analysis Project (GTAP) produced, the power-sector-only approach requires a carbon price for electric utilities that is almost twice the economy-wide carbon price that would achieve the same cumulative emissions.

3.3 Data and methodology

This study uses the CGE model, a very dynamic model, to analyze problems in income distribution. According to Bourguignon and Bussolo (2013), most of the CGE disaggregated macroeconomic models detail several household groups distinguished by their production factors. There are two critical components in the CGE database model. First, the Social Accounting Matrix (SAM) reports the entire value of economic transactions over a certain period, usually in one year. SAM data are organized logically, with rows and columns visually representing all transactions as circular flows of national income and expenditure in the economy. The second component is the elasticity parameter which describes the responsiveness of producers and consumers to changes in prices and relative incomes.

3.3.1 Data

3.3.1.1 SAM Data

The data to be used is in the Indonesia Macro SAM 2018 released by the International Food Policy Research Institute (IFPRI) in 2021 (Pradesha, 2021), which consists of four standards nexus of 42 activities and commodities as shown in Table 3.1, Factors of production (i.e., Labor, Land, and Capital), Households that separate national populations into ten representative household groups, and other accounts which include the transaction costs of moving goods between producers, domestic markets, and national borders, as well as the various indirect taxes imposed on marketed commodities. The most important is the household-level survey data from the microdata of Indonesia's National Socio-Economic Survey (SUSENAS) obtained from the Central Bureau of Statistics (BPS) and has been disseminated to several ministries/agencies, including the Directorate General of Taxes (DGT).

Table 3.1: Standard Nexus SAM Activities and Commodities

Code	Description	Code	Description
maiz	Maize	text	Textiles, clothing and footwear
rice	Rice	wood	Wood and paper products
ocer	Other cereals	chem	Chemicals and petroleum
puls	Pulses	nmet	Non-metal minerals
oils	Oilseeds	metl	Metals and metal products
root	Roots	mach	Machinery, equipment and vehicles
vege	Vegetables	oman	Other manufacturing
sugr	Sugarcane	elec	Electricity, gas and steam
toba	Tobacco	watr	Water supply and sewage
cott	Cotton and fibers	cons	Construction
frui	Fruits and nuts	trad	Wholesale and retail trade
coff	Coffee, tea and cocoa	tran	Transportation and storage
ocrp	Other crops	hotl	Accommodation and food services
catt	Cattle and raw milk	comm	Information and communication
poul	Poultry and eggs	fsrv	Finance and insurance
oliv	Other livestock	real	Real estate activities
fore	Forestry	bsrv	Business services
fish	Fisheries	padm	Public administration
mine	Mining	educ	Education
food	Processed foods	heal	Health and social work
beve	Beverage and tobacco	osrv	Other services

Source: IFPRI, 2021

3.3.1.2 The Electricity/energy data

I am using Indonesia's Electric State-Owned Company (PT PLN) for electricity prices from 2018 to 2020. These datasets consist of fixed and variable Operating and Maintenance (O&M) Costs and Marginal Costs for different sources of energy. In this paper, I will use fossil fuels like coal and renewables, like solar, which are dominant in the eastern part of

Indonesia. Table 3.2 shows the power plant and the corresponding power sources in the Timor System network.

Table 3.2: Power plant in Timor System

Power Source	Name of Power Plant	Capacity Netto
Coal	PLTU Bolok	$2 \times 15{,}00$ MW
Coal	PLTU IPP SMSE	$2 \times 15{,}00$ MW
MFO	PLTD Cogindo	$5 \times 8{,}00$ MW
HSD	PLTMG Kupang Peaker	$5 \times 9{,}49$ MW
Solar	PLTS IPP Atambua	1 MWp
HSD	ULPL Kupang	9,51 MW (Total 5 Engine)
HSD	ULPL Atambua	2,61 MW (Total 5 Engine)

Source: PLN, 2021

3.3.2 Methodology

3.3.2.1 Key features of the model

In this study, I will use an extension of the CTAP Model introduced by Cai and Arora (2015) to model the disaggregation of electricity sectors in Indonesia. Also, I will use the CGE Model to calibrate Indonesia's SAM data into the integrated CGE Model for Indonesia from 2018 to 2020, so it will account for the change in electricity prices. It is similar to the ORANI-G model as introduced by Horridge (2000). This model is commonly used in Indonesia's Energy prices effect on the economy and allows substitution between types of energy, such as fossil and renewable energy (wind and solar), and between primary input factors (Capital, Labor, and Land) and energy. This model uses 38 industries and 43 commodities with a detailed energy sector. Energy commodities include coal, natural gas, fuel, and renewable energies such as wind and solar.

CTAP model has been adapted by having multiple households from the income or demand side of the model and the income side of the families. It doesn't have the technology bundle like in the CTEM model, as introduced in Cai and Arora's paper. However, it allows for substitution between a primary factor composite (labor, capital, and fixed-factor energy resources) and a fuel composite (coal, petroleum, and gas). In this paper, due to the limited data on Indonesia's energy prices, the modified CTAP model only considers fossil fuels like coal technology and renewables like solar. Also, it follows standard economic theory and allows for different assumptions about substitutability between technologies. The model will specify the uptake of clean energies through substituting fossil fuels for capital and fixed-factor energy resources. Figure 3.2 shows the diagram of the CTAP model that uses a combination of primary factors and fossil fuels in the Generation (GEN) part.

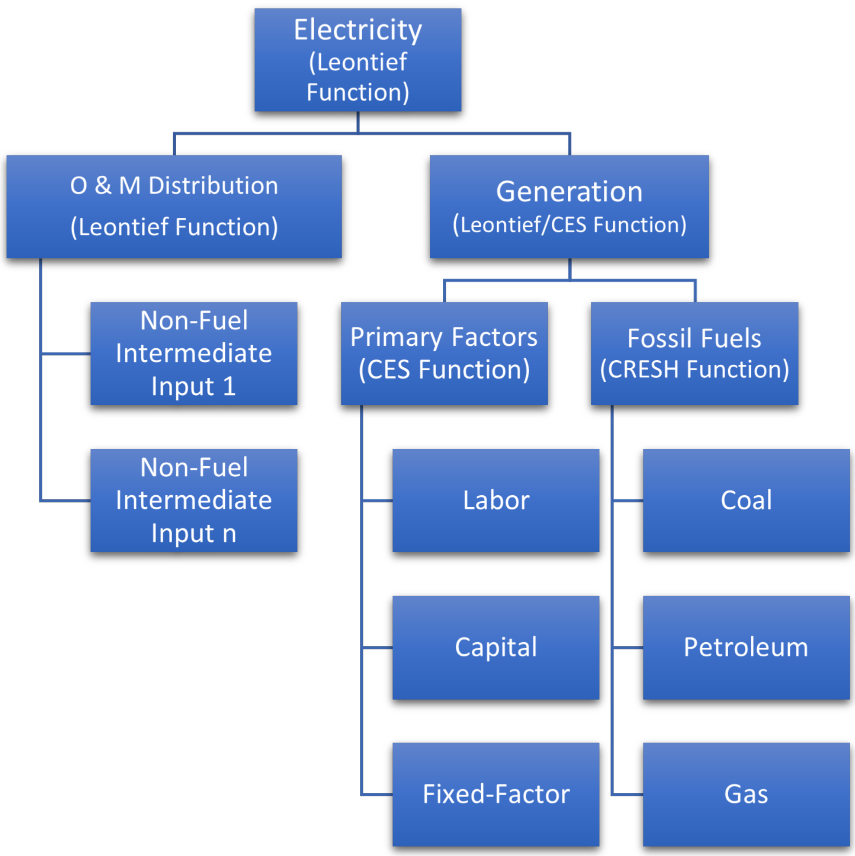

Figure 3.2: Production Structure of Electricity in CTAP (Modified from Figure 4 in Cai and Arora (2015))

This research will also include an element of tax incentives, namely PTC, which is the focus of the analysis of the economics of the NRE industry.

Next, following Cai and Arora (2015), the model assumes that electricity is a homogenous good produced by aggregating Generation (GEN) and O&M and Distribution (OMD), as shown in Figure 3.2 above. GEN is the crucial component of this setup that allows for a bundle of heterogeneous and competing electricity generation technologies. OMD combines TD and OH, representing all non-technology-specific activities, such as construction and daily maintenance. OMD aggregates intermediate inputs used to produce electricity but not specific to a particular generation technology. The complementarity of GEN and OMD reflects that electricity generators are connected to end-users through electricity transmission grids. Fossil Fuels will use the structure of the Constant Ratios of Elasticities of Substitution, Homothetic (CRESH) function, introduced by Hanoch (1971), which allows for differing substitution levels between electricity generation technologies. The GEN activity distinguishes between multiple technologies that are substitutes. However, this approach uses a constant elasticity of substitution (CES) production function that assumes the degree of substitution between competing technologies is the same.

The mathematical details are as follows. At the top level, electricity production (E) is a Leontief function of the GEN activity (X) and OMD activity (Y):

$$E = \min\{A_1 \cdot X, B_1 \cdot Y\} \tag{3.1}$$

where A_1 and B_1 are scale factors representing the efficiency of each activity, and min is the minimum operator. This operator indicates that the two activities are non-substitutable, so the outputs of GEN and OMD are combined in fixed proportions.

The first term of Equation (3.1) represents the GEN function. The X units of electricity can be generated by a bundle of technologies (Q_i) through a CRESH production function. The production function is implicit but satisfies the following:

$$\sum_i \left(\left(\frac{Q_i}{X} \right)^{d_i} \cdot \frac{D_i}{d_i} \right) = \kappa \tag{3.2}$$

In this equation, d_i is a parameter with a value less than 1 but not equal to zero. Each D_i parameter associated with a particular technology is positive, and the D_i values and κ are normalized such that $\sum_i D_i = 1$. In the special case where $d_i = d$ for all i, the CRESH function collapses to the CES function:

$$X = \frac{1}{d\kappa}\left[\sum_i \left(Q_i^d \cdot D_i\right)\right]^{1/d} \tag{3.3}$$

The next step is the optimization problem. Given the amount of total generation (X) and production costs for each technology (P_i), the electricity producer chooses demand for each technology (Q_i) to minimize total cost $\sum_i Q_i(P_i - \tau) = C$, subject to Equation (3.1). The linearized solution to this problem yields:

$$q_i = q_X - a_i\left((p_i - \tau) - p_X^*\right) \tag{3.4}$$

where $a_i = \frac{1}{1-d_i}$, $p_X^* = a_i \cdot S_i \cdot (p_i - \tau)$, and $S_i = \frac{Q_i \cdot (P_i - \tau)}{\sum_i Q_i \cdot (P_i - \tau)}$ (the cost share of technology i), where τ is the Production Tax Credit. Here, p_i, q_i, and q_X are the percentage changes of P_i, Q_i, and X, respectively. Equation (3.4) shows that demand for each technology depends upon total demand for generation, production costs for each technology, and various parameters.

It is also necessary to model the technology production for the factor composite (F_i) and intermediate inputs (G_i):

$$Q_i = \min\{A_2 \cdot F_i, B_2 \cdot G_i\} \tag{3.5}$$

In Equation 3.5, A_2 and B_2 are the scale factors representing the efficiency of each activity, and $\min$ is the minimum operator. The factor composite is an aggregate of labor, capital, and the fixed-factor energy resources (if applicable).

Each of the intermediate inputs (G_i) is an aggregate of imported and domestic goods. The aggregation is represented by a CES function, which allows substitution between imported and domestic goods, G_i^{Imp} and G_i^{Dom}:

$$G_i = \left[\rho_{\text{Dom}} \left(G_i^{\text{Dom}}\right)^{\frac{\rho-1}{\rho}} + \rho_{\text{Imp}} \left(G_i^{\text{Imp}}\right)^{\frac{\rho-1}{\rho}}\right]^{\frac{\rho}{\rho-1}} \tag{3.6}$$

Here, ρ is commonly known as the Armington elasticity of substitution between imported and domestic goods, and ρ_{Dom} and ρ_{Imp} are budget share parameters.

The OMD activity, shown in Figure 3.1, can be modeled as a Leontief function of non-technology-specific intermediate inputs (G):

$$Y = \min\{B_3 \cdot G\} \tag{3.7}$$

Here, B_3 is a vector of scale factors representing the efficiency of each intermediate input, and Min is the minimum operator. As before, the intermediate inputs are aggregates of domestic and imported goods.

After calibrating all the numbers into all the equations, the challenge is to allocate the output and inputs of the electricity sector into technologies in a manner consistent with a CGE model's social accounting matrix. Choosing the appropriate level of output and input detail for power generation technologies in each region of the model is particularly challenging. For example, on the input side, the challenge is deciding the appropriate weights for each factor of production and technology-specific intermediate input.

So, the next process will be to match Indonesia's SAM model to the electricity data and narrow it down into region-specific datasets for the Timor System Region. The most important thing is to obtain the elasticity of substitution between fossil fuel and renewable sources and the portion of labor or employment attributed to each energy source.

3.3.2.2 Assumptions

The CGE model is a widely used tool for analyzing the economy-wide effects of policy changes. It allows for examining the complex interactions among various economic agents and sectors. In this study, I focus on the impact of PTC on key macroeconomic variables such as employment, factor income of labor, and household consumption. Before presenting the results, I first describe the key assumptions underlying the model and the calibration process used to ensure that the model is consistent with the actual economy.

1. *Perfect competition*: The model assumes that all firms and households are price-takers and have no market power.

2. *Full employment*: The model assumes that all factors of production are fully employed in the economy.

3. *Static analysis*: The model assumes that the economy is in a steady state and does not take into account any dynamic effects or adjustments that may occur over time.

4. *Perfect information*: The model assumes that all agents have perfect information about the economy and the policy changes being analyzed.

5. *No external shocks*: The model assumes that no external shocks or unexpected events could affect the economy during the analysis period.

3.3.2.3 Model Calibration

The accuracy of any economic model's predictions is highly dependent on its calibration. In this section, I discuss the calibration process for my CGE model, which I use to analyze the economic effects of applying a PTC in the electricity sector. The calibration process involves estimating the model's parameters based on available data to reflect the real-world economy accurately. I begin by describing the methods I used to estimate the model parameters.

$$QVA_a = iva_a \cdot QA_a \tag{3.8}$$

where QVA_a represents the demand for value-added, iva_a denotes the quantity of value-added per activity unit, and QA_a signifies the quantity (level) of activity.

$$PA_a \cdot (1 - tva_a) \cdot QA_a = PVA_a \cdot QVA_a + PINTA_a \cdot QINTA_a \tag{3.9}$$

where PA_a represents the activity price (gross revenue per activity unit), tva_a denotes the tax rate of the activity, $PINTA_a$ signifies the aggregate intermediate input price for activity a, and $QINTA_a$ signifies the quantity of aggregate intermediate input.

3.3.2.4 Simulation Procedures

The modeling process will be conducted as follows. Firstly, the simulations will be based on assessing the impact of the Production Tax Credit (PTC) on the Total Factor Productivity (TFP) increase within the renewables sector. To estimate the economic development effects, I will refer to the technical report by Lantz (2009) on Wind Energy in Nebraska, which provides insights into the anticipated impacts of constructing and operating 7,800 MW of new wind power in Nebraska. This level of development aligns with the Department of Energy's (DOE) goal of achieving 20% Wind Energy by 2030.

In their analysis, Lantz (2009) focuses on the potential support of 20,600 to 36,500 annual full-time equivalents (AFTE) through developing and constructing approximately 7,800 MW of wind energy in Nebraska by 2030. By incorporating this information into our simulation, I can assess the potential employment impacts resulting from the deployment of renewable energy sources and the associated TFP increase facilitated by the PTC.

Secondly, I will explore the possibility of observing the effects of increasing TFP to 30% or higher. This higher TFP increase allows us to examine the potential economic and employment outcomes under more optimistic scenarios. By considering different levels of TFP increase, we can analyze the sensitivity of the results and understand the range of potential impacts on various economic indicators.

The TFP will impact the macroeconomic condition in these several ways: First, I will extend Equations 3.8 and 3.9 to get the shift parameter for the CES activity production function in Equation 3.11. Equation 3.10 constructs the necessary formula to form the TFP growth rate:

$$\begin{aligned} \text{FIN\_TFPGR}(A, RG, XC, TC) = \frac{100}{\text{BASE\_TFP}} + \sum_{(T,TP)} (\text{XT\_TFP}(XC, TC, T)) \\ \cdot(\text{SIM\_TFP}(A, RG, XC, T, TP)) \cdot \frac{1}{100} \end{aligned} \tag{3.10}$$

where: FIN_TFPGR is the TFP growth rate for each activity (A), region (R), i.e., urban and rural, active simulation for every X value (XC), and each active period T (TC), BASE_TFP is the baseline sectoral TFP growth projections, XT_TFP is the sectoral TFP growth projections for each active simulation for every X value (XC), and each active period T (TC), and SIM_TFP is the simulation sectoral TFP growth projections for each activity (A), region (R), i.e., urban and rural, active simulation for every X value (XC), each active initial period T (TC), and end of periods T (TP).

Equation 3.11 formulates the shift parameter for the CES production function using Equation 3.10:

$$\alpha_{va}(A, RG) = \alpha_{va}(A, RG) \cdot (1 + \text{FIN\_TFPGR}(A, RG, XC, TC)) \tag{3.11}$$

where α_{va} is the shift parameter for the CES activity production function.

Calculating the shift parameter based on the quantity of Value-Added for each activity and region will calculate the value-added demand (QVA) and share parameter for the CES activity production function (δ_{VA}) in Equation 3.12.

$$\alpha_{va}(A, RG) = \left(\frac{QVA_0(A, RG)}{(\sum_F \delta_{VA}(F, A, RG) \cdot QF_0(F, A, RG))^{-\rho_{VA}(A,RG)}} \right)^{-\frac{1}{\rho_{VA}(A,RG)}} \tag{3.12}$$

where QVA_0 is the initial quantity of aggregate value added for each activity (A) and region (R), δ_{VA} is the share parameter for the CES activity production function, QF_0 is the initial quantity demanded of factor production ($fprd$) of Capital ($fcap$), Land ($flnd$), and Labor ($flab$) from activity (A), and ρ_{VA} is the elasticity of substitution of activity (A) production.

Calculating the CES Production Function for the Quantity of Value-Added in Equation (3.13) for each activity and region using Equations 3.10, 3.11, 3.12:

$$\text{CESVAPRD}(A, RG) = \Bigg(\sum_{F \in QF_0(F,A,RG)} \delta_{va}(F, A, RG) \cdot \big(fprd(F, A, RG) \cdot QF(F, A, RG) \cdot UF(F, A, RG)\big)^{-\rho_{VA}} \Bigg)^{-\frac{1}{\rho_{VA}}} \tag{3.13}$$

where CESVAPRD is the CES value-added production function for each activity (A) and region (R), $fprd$ is the factor-specific productivity, and UF is the factor utilization rate, where 1 is fully utilized.

Finally, those four updated equations will be used to calculate TFP simulated effects in section 3.4. The First Order Condition (FOC) of Equation 3.13 w.r.t. QVA in Equations 3.8 and 3.9 will result in Equation 3.14:

$$\begin{aligned} \text{CESVAFOC}(F, A, RG) = {} & PVA(A, RG) \cdot (1 - tva(A, RG)) \cdot QVA(A, RG) \\ & \cdot \sum \delta_{va}(FP, A, RG) \cdot (fprd(FP, A, RG) \cdot QF(FP, A, RG) \\ & \cdot UF(F, A, RG))^{-\rho_{va}} \cdot \delta_{va}(F, A, RG) \cdot (fprd(F, A, RG))^{-\rho_{va}} \\ & \cdot (QF(F, A, RG) \cdot UF(F, A, RG))^{-\rho_{va(A,RG)-1}} \end{aligned} \tag{3.14}$$

where: CESVAFOC(F, A, RG) is CES value-added first-order condition, PVA is value-added price for each activity (A) and region (RG)

While this simulation provides valuable insights into the potential effects of TFP increases on the macroeconomic condition, it is essential to acknowledge that the modeling approach has limitations. The assumption of a fixed TFP growth rate and its direct impact on the CES activity production function may not fully capture the complexities and dynamics of real-world economies. Factors such as technological advancements, changing market conditions, and institutional influences are not explicitly accounted for in this model, which could lead to an incomplete understanding of the TFP-macroeconomy linkage.

The key parameters to calculate the CGE simulation are shown in Table 3.3. These parameters are based on the 2018 Indonesia macroeconomics indicator released by the competent authority.

Table 3.3: Parameters/Variables for calculating the increase of TFP due to the effect of the application of the Production Tax Credit

Parameters/Variables	Values	Notes
t_{va}	10%	Indonesia's VAT rate
SIM_TFP	20% and 30%	TFP growth for the first and second simulation
ρ_{VA}	-0.5	The elasticity of substitution for most activities (A)

Source: BPS, 2018

3.4 Quantitative results

3.4.1 Overview of the simulation result

The overall objective of the macro simulation of this particular government subsidy is to see the effect of the PTC on renewables by simulating how it will affect the economy as a whole. Indonesia aims to increase renewable energy production by projecting that the power generation capacity, especially wind and solar power, can reach 106,354 gigawatt hours (GWh) in 2030.[8] A long-term plan has been laid to achieve the net-zero emission target by 2060. For example, Indonesia will gradually retire the coal-fired power plants with a steam power plant monetization scheme. That would replace the conventional coal power plant with the variable renewable energy power plant. However, the high investment cost to build the new power plant would hinder more investors from involving in this multiyear project. The most significant concerns are the cost in the early production stage, including the tax and hard-to-get loans from lending institutions, among other things.[9]

The US PTC is a federal incentive included under Section 45 of the US tax code that reduces the cost of renewable energy projects.[10] The PTC provides a corporate tax credit of up to 1.3 cents/kWh for electricity generated from landfill gas (LFG), open-loop biomass, municipal solid waste resources, and small irrigation power facilities, or up to 2.6 cents/kWh for electricity generated from wind, closed-loop biomass, and geothermal resources. The credit is suitable for ten years after the equipment is in service. The credit is available for eligible technologies such as wind, solar, geothermal, and biomass. The PTC has been extended several times since its inception in 1992. For developing countries like Indonesia, this would boost the economy-wide sectors in two ways. First, as of the US experience on the requirement of the business that qualifies for this incentive, the wind power sector must meet the prevailing wage and apprenticeship requirements for all laborers and mechanics employed by the taxpayer to receive the full production tax credit of 2.6 cents per kilowatt-hour.[11] Solar energy projects must begin construction before January 1, 2025, to be eligible for the production tax credit. Unfortunately, a few jobs and power plant projects

---

[8]See https://databoks.katadata.co.id/datapublish/2022/02/18/kapasitas-ebt-diproyeksikan-capai-106354-gwh-pada-2030

[9]See Katadata White Paper, "Kolaborasi Menuju Transisi Energi Berkelanjutan", July 2020 (translated)

[10]See https://www.epa.gov/ for more information

[11]Inflation Reduction Act (IRA), signed by President Biden on August 16, 2022, has extended to wind projects that begin construction before the end of 2024. Before the IRA, PTC for wind projects was available only to facilities that began construction before Jan. 1, 2022

in the renewable energy sector were created before 2022 in Indonesia. There was also negative growth in renewable energy investment in several countries in Asia, including Indonesia, during this period, as pointed out in Figure 3.3. As mentioned in Section 3.3, the increase in TFP from the electricity sectors due to applying PTC will lead to a decrease in the relative price of electricity and, thus, an increase in demand. In this simulation, I make two scenarios where TFP in the electricity sector increase by 20% and 30%, as suggested by several works of literature. Second, in this simulation, I will discuss the distribution results of the analysis of income distribution patterns in the various households' employment sector.

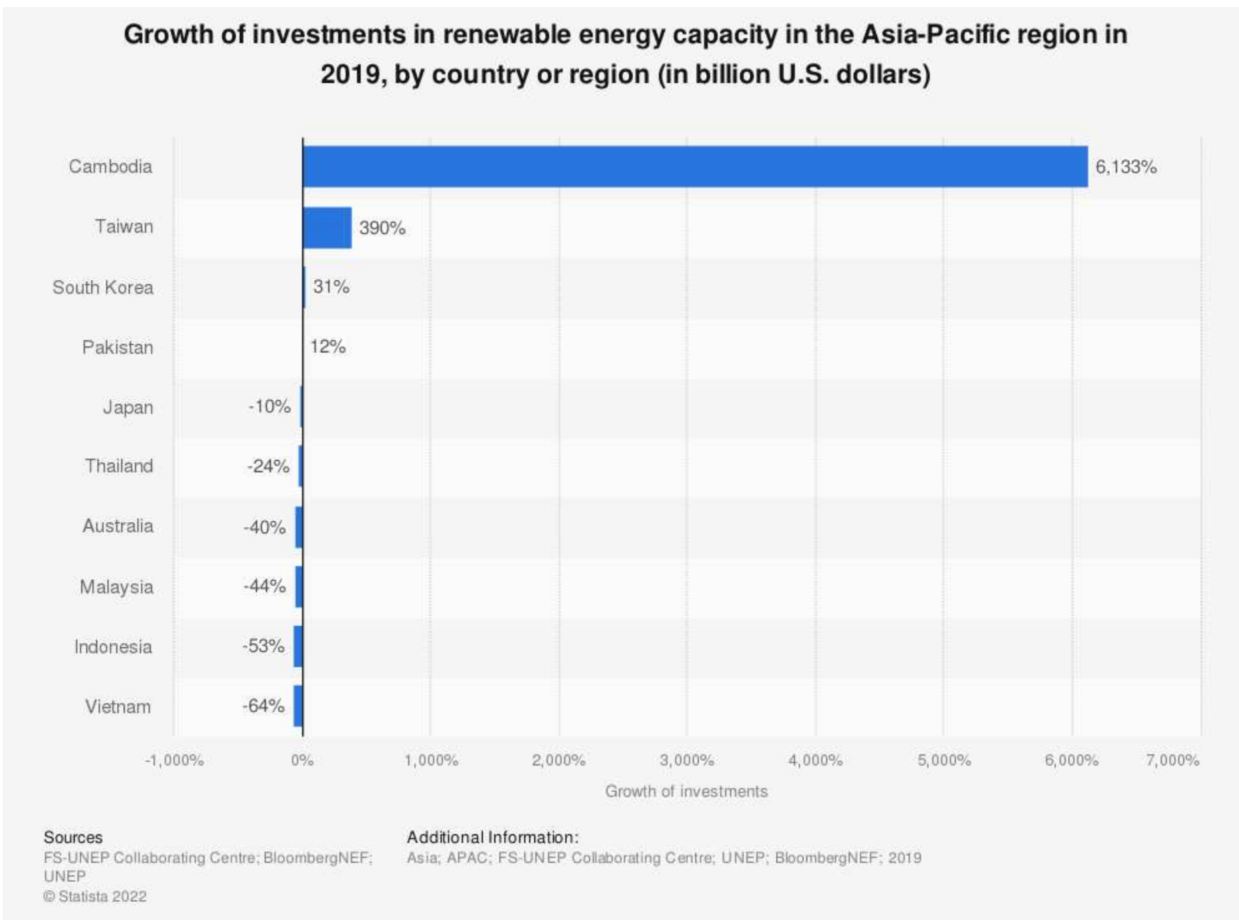

Figure 3.3: Growth of Investment in Renewable Energy Capacity in Asia-Pacific Region, 2019

3.4.2 The results on the impact of PTC on electricity prices

In this section, I simulate the effect of applying the production tax credit (PTC) to electricity prices if electricity producers qualify to meet the investment goal set by policy-makers. I consider two scenarios: (i) a 20% increase in total factor productivity (TFP) in the electricity sector and (ii) a 30% increase in TFP in the same sector. The simulation results are presented in Figure 3.4, which shows the projected electricity prices for both scenarios.

Choosing 2018 as the base year enables me to establish a baseline and capture the prevailing trends and conditions in Indonesia's electricity sector, given its historical path and energy transition roadmap leading up to 2030. These simulation results reveal a significant decrease in electricity prices, with the most substantial reduction occurring in 2025 for both scenarios, ranging from 63% to 65%. Importantly, I find that the gap in the decline of electricity prices between the two scenarios will not be too large by the end of the observation period in 2030. A similar study by Hwang and Lee (2015) suggests that since electricity demand's price elasticity tends to be low, convergence may not be guaranteed during an iterative process between scenarios. Additionally, it is worth noting that the electricity market in Indonesia is unique, and the results of this study are subject to policy changes that could affect market structure and pricing. Soummane et al. (2019) support these findings by demonstrating that regulated electricity prices in emerging G20 countries tend to converge to average prices. These results suggest that a production tax credit could significantly decrease electricity prices, with relatively small differences between scenarios by 2030.

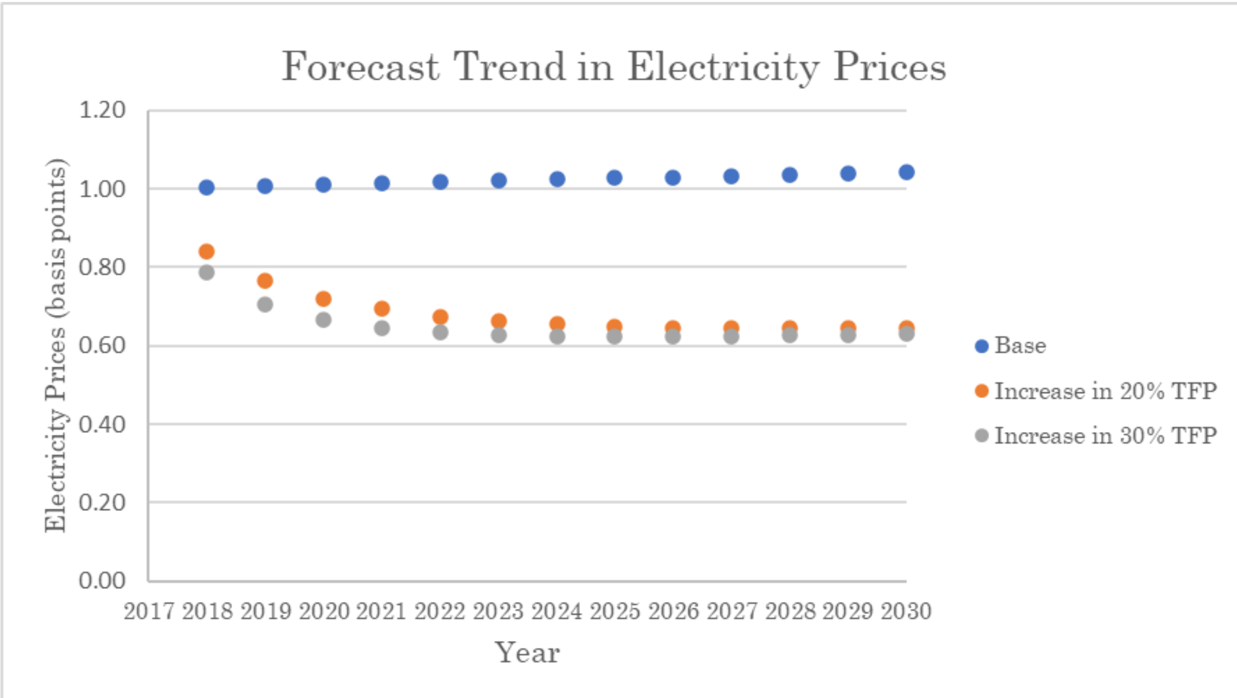

Figure 3.4: The decrease in electricity prices due to the impact of the PTC

Table 3.4 shows the results of our sensitivity analysis on the production tax credit, with three scenarios: a baseline scenario with no production tax credit with 1% inflation each year and two policy scenarios that lead to TFP increases of 20% and 30%. The table displays the projected trend of electricity tariffs in both policy scenarios.

The sensitivity analysis results indicate that the production tax credit leads to a significant increase in electricity supply, as renewable energy investment is incentivized. The increase in supply leads to a decrease in the marginal cost of production, reducing the electricity tariffs.

It is important to note that the assumptions and data used in this simulation are subject to certain limitations, and I make several assumptions for interpreting the results. First, the electricity market is in perfect competition, meaning that markets for electricity generation and transmission are perfectly competitive, which means that prices are set at the marginal cost of production. While this is true for the developed countries, Indonesia's electricity market is entirely different in terms of the market structure, where electricity prices are determined by the sole entity appointed by the central government. Thus, the results of the estimated path of the electricity prices are conditional upon the government policy on the market structural change within the country. Second, price determination in the electricity market is a complex process that is influenced by various factors such as fuel costs, transmission and distribution costs, and policy interventions. While I have attempted to account for these factors in our analysis, it is possible that the results may not fully capture the complexities of the Indonesian electricity market.

Table 3.4: Forecast of Electricity Prices Trend from 2018 to 2030 due to the application of TFP in Timor System

Year	Base Tariff ($/kWh)	20% increase in TFP ($/kWh)	30% increase in TFP ($/kWh)
2018 (Base)	0.1954	0.1642	0.1541
2019	0.1962	0.1500	0.1385
2020	0.1969	0.1419	0.1313
2021	0.1976	0.1370	0.1276
2022	0.1982	0.1338	0.1258
2023	0.1987	0.1318	0.1249
2024	0.1993	0.1305	0.1246
2025	0.1998	0.1298	0.1248
2026	0.2004	0.1295	0.1251
2027	0.2009	0.1296	0.1256
2028	0.2015	0.1298	0.1263
2029	0.2020	0.1302	0.1271
2030	0.2026	0.1308	0.1279

Source: Author's calculation from the attachment of the Indonesia's Minister of Energy Regulation number 55 K/20/MEM/2019

3.4.3 The results of the analysis of income distribution patterns in the households and employment sector

In this section, I present a detailed analysis of income distribution patterns in the Households and Employment sector, which is a crucial aspect of assessing the impact of policy changes on the overall welfare of the economy. The distributional impact of policy changes on different income groups is an essential consideration for policymakers. This analysis aims to shed light on the effects of the policy scenarios on various income groups.

To evaluate the impact of policy changes on income distribution, I use the same scenarios as in the previous section and examine the effects of the policy changes on the income of different households and employment sectors. The results presented here will provide valuable insights into how policy changes can affect income distribution in the economy and inform policymakers in their decision-making processes.

3.4.3.1 Implication on the household consumption

In this section, I analyze the implications of policy changes on household consumption, examining the effects of price and income level changes on consumption patterns and exploring the distributional impacts across different income groups. Figure 3.5 illustrates the Household income expenditure for a selected population in rural and urban regions. The per capita consumption quintiles further disaggregate rural and urban households. These quintiles are defined at the national level, ensuring comparability and equal representation of each quintile's population, corresponding to one-fifth of the national population.

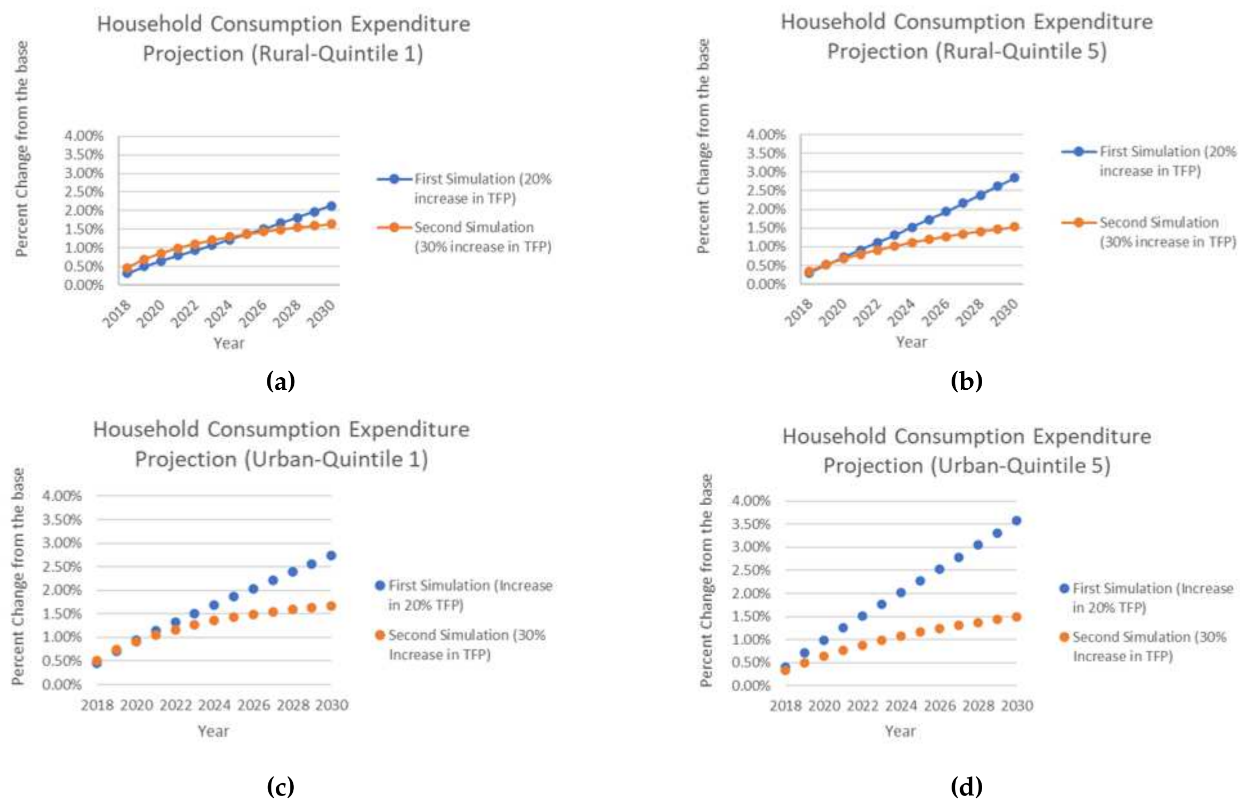

Figure 3.5: Household income expenditure from different regions and groups of the national population

The sensitivity analysis reveals that applying the Production Tax Credit (PTC) on renewable energy has divergent effects on consumption expenditure trends between rural and urban areas in the Timor System. Figure 3.5a and 3.5c depict the number of households in sparsely populated rural areas, where most families work as seaweed farmers and heavily rely on electricity generated from coal-fired power plants. Figure 3.5b and 3.5d represent the urban population.

The analysis demonstrates that the consumption expenditure trend for the first quantile in rural areas, under the PTC scenario, is relatively lower compared to urban areas. The trend slope appears flatter during 2018-2030, indicating slower consumption expenditure growth. These findings suggest that the PTC policy may have a limited impact on enhancing the welfare of the least well-off households in rural areas. Conversely, the consumption expenditure trend for the urban population exhibits rapid growth during the initial seven years until 2025, followed by stabilization in subsequent years. That indicates a significant impact of the PTC policy on urban households, who likely possess a greater capacity to invest in renewable energy and benefit from reduced electricity tariffs. However, the initial increase in consumption expenditure could lead to higher inflation and potentially adverse welfare effects for certain urban households.

Moreover, implementing the PTC increases Total Factor Productivity (TFP) growth within the electricity sector. It will lead to enhanced productivity and efficiency in renewable energy generation. This initial boost in TFP growth contributes to an overall rise in income expenditure across rural and urban areas.

However, as time progresses, the effects of the increased TFP growth may gradually diminish or encounter certain limitations. In the case of the 30% TFP growth scenario, it is observed that the growth rate in income expenditure eventually slows down and falls below that of the 20% TFP growth. This phenomenon can be attributed to factors specific to the electricity sector and the broader economic landscape.

Renewable energy generation capacity saturation within the electricity sector plays a role in this context. As the renewable energy infrastructure expands and reaches a certain level of development, the potential for further growth becomes constrained, resulting in diminishing returns regarding the additional benefits derived from higher TFP growth.

Furthermore, changes in market dynamics and economic factors influence the growth rate of income expenditure. Factors such as fluctuations in energy demand, shifts in consumer preferences, or changes in policy frameworks can impact the overall economic performance of the electricity sector. Consequently, these factors can influence the profitability and competitiveness of renewable energy technologies, hence affecting the growth rate of income expenditure associated with the industry.

Additionally, the differential impact between rural and urban areas can be attributed to disparities in industry structures, labor market dynamics, and specific policy contexts.

Urban areas typically possess a more diverse and developed economic base, which renders them more resilient and adaptable to changes in TFP growth. Conversely, rural areas exhibit different dependencies and vulnerabilities with specific economic activities such as seaweed farming, leading to distinct consumption expenditure trends.

3.4.3.2 The implication to the employment and factor income of labor

Given the significant role of labor and employment in producing renewable energy, it is essential to examine the effects of this policy measure on the labor and employment factor income. Specifically, I analyze the impact of the PTC on the employment levels of education and evaluate its effect on the overall welfare of the economy.

In this section, I present the implications of the production tax credit policy on labor employment and factor income. To assess these implications, I first defined three types of labor: Low Skill, which has no basic education; Medium Skill, which has education less than a college degree; and High Skill, which has a college or professional degree (ILO, 2014). Figure 3.6 shows the simulation results for the employment of each type of labor under both scenarios. As shown in the graph, the employment of each type of labor declines overall in both scenarios. This is due to the relative increase in the price of capital-intensive goods, which leads to a shift in production towards capital-intensive industries. As a result, labor-intensive industries experience a decrease in demand for labor, causing a decline in the employment of each type of labor.

However, it is worth noting that this result differs somewhat from other CGE analyses. For example, Böhringer et al. (2013) analyzed the German economy's overall employment and welfare impacts of alternative financing subsidies for renewable energy capacity creation. They found that the decline in employment is more significant for low-skilled labor, reflecting the sectoral shift towards capital-intensive industries that require higher-skilled workers. The production tax credit policy will likely hurt employment, particularly for low-skilled workers. It is important to note that this interpretation assumes that no in and out-migration would affect the number of populations during the observation period.

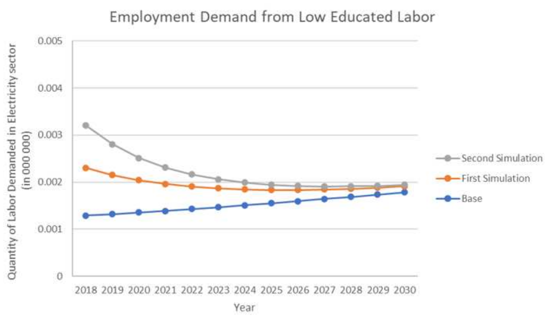

(a)

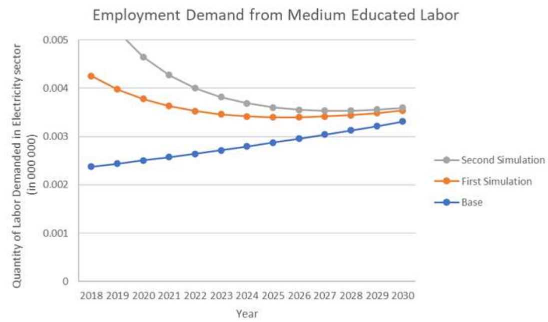

(b)

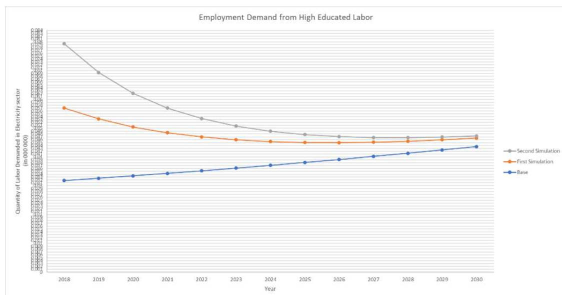

(c)

Figure 3.6: Employment demanded in the electricity sector

Notably, the decline in employment within the two scenarios will converge almost the same amount by the end of the observed period. This result is identical to the previous effect on the simulated decrease in electricity prices, which indicates that convergence may not be guaranteed during an iterative process between scenarios.

However, there are different results from the agricultural sector, such as the Maize sector. The Maize sector, in particular, has experienced a surge in demand for employment due to the production tax credit and the subsequent increase in TFP within the electricity sector. This boost in employment opportunities has profoundly impacted the overall agricultural industry, leading to a more robust and thriving Maize sector.

Furthermore, the rise in TFP within the electricity sector, which was facilitated by the implementation of the production tax credit, has had a positive spillover effect on the Maize sector, as shown in Figure 3.7. This increased productivity has allowed for more efficient resource allocation and production processes within the agricultural sector, ultimately leading to improved outcomes, such as increased crop yields and enhanced overall economic performance.

Therefore, it can be concluded that applying the production tax credit has not only resulted in positive outcomes for the electricity sector but has also triggered notable improvements in the agricultural industry, particularly in the Maize sector. The increase in employment demand and the rise in TFP within the electricity sector have played instrumental roles in driving these favorable outcomes, contributing to a more prosperous and dynamic agricultural sector.

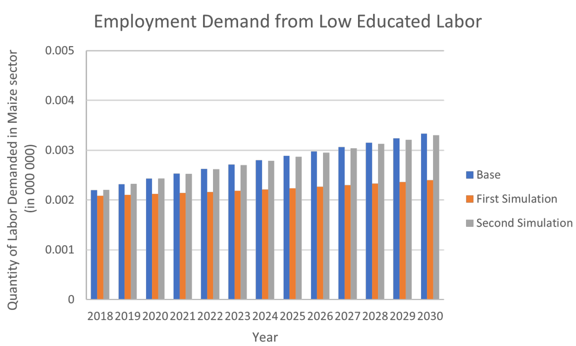

(a)

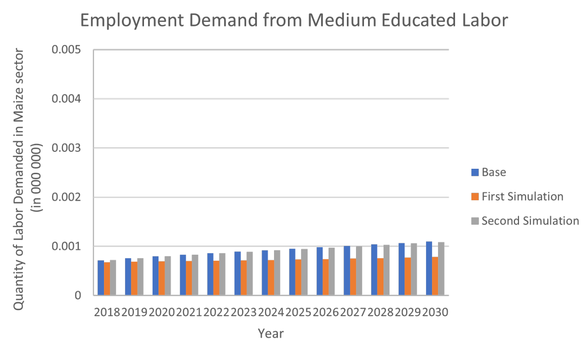

(b)

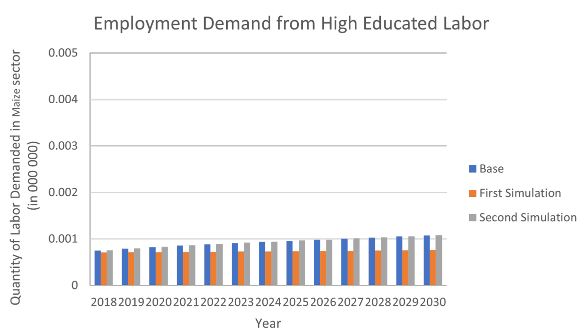

(c)

Figure 3.7: Employment demanded in the Maize sector

Next, I further analyze the impact of the PTC on the factor income of labor in different education levels of employment. Figure 3.8 reveals that highly educated labor's income significantly increases for both scenarios. This finding is unsurprising as most educated workers tend to be employed in industries that benefit the most from the PTC. However, the factor income of low and medium-skilled labor slightly decreases for both scenarios, indicating that the PTC policy may not be favorable for all types of labor in terms of income. These results are consistent with previous CGE studies, such as the analysis by Al-Riffai et al. (2015) on the impact of renewable energy subsidies on the economy-wide sectors. They found that the subsidies tend to favor high-skilled workers, while low and medium-skilled workers may experience a decline in their wages. The middle of the urban income distribution typically benefits the most since these quintiles rely more heavily on labor wages for their incomes. Moreover, these households generally are endowed with semi-skilled and high-skilled labor, used fairly intensively in the renewable equipment manufacturing sectors (such as operators and technicians).

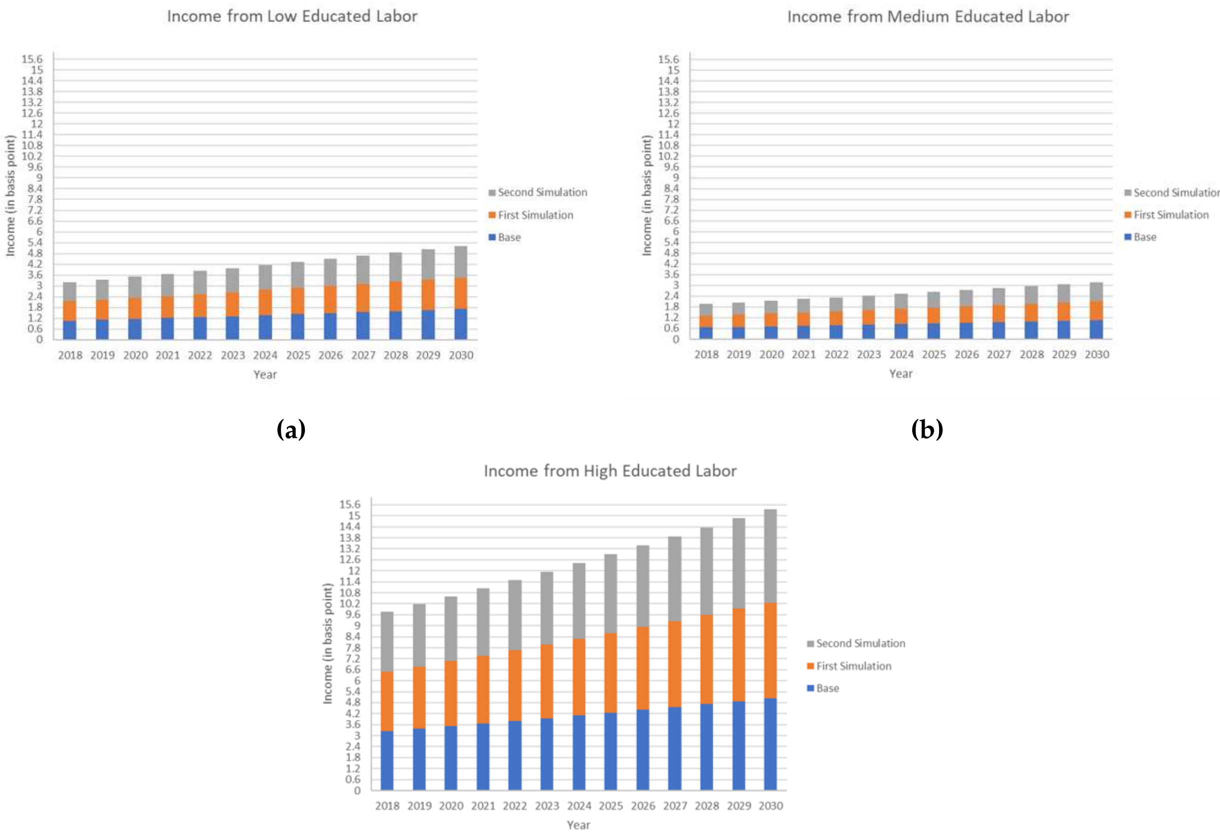

(a) (b) (c)

Figure 3.8: Factor Income from different type of labor

Overall, the implications of the PTC on the factor income of labor highlight the need for policymakers to carefully consider the distributional impacts of renewable energy policies and explore ways to mitigate any adverse effects on low and medium-skilled workers.

3.5 Conclusion and policy recommendation

In this research, the simulation results indicate that implementing a production tax credit (PTC) for the electricity sector can significantly decrease electricity prices. The study considers two scenarios with different total factor productivity (TFP) increases, and both scenarios show substantial reductions in electricity prices, particularly in 2025. The results suggest that the gap between the two scenarios' price declines diminishes over time, indicating that convergence may not be guaranteed during the iterative process between scenarios.

However, it is important to note that the findings are subject to certain limitations and assumptions. The electricity market in Indonesia has a unique structure, and the results depend on potential policy changes that could affect market structure and pricing. Additionally, the impacts of the PTC on consumption expenditure and labor employment differ between rural and urban areas. The policy has limited effects on enhancing the welfare of the least well-off households in rural areas. In contrast, urban households benefit more due to their greater capacity to invest in renewable energy. However, initial increases in consumption expenditure could lead to higher inflation and potentially adverse welfare effects for certain urban households.

Furthermore, the analysis highlights the importance of considering the saturation of renewable energy generation capacity and changes in market dynamics over time. The effects of increased TFP growth may gradually diminish, and other factors, such as energy demand fluctuations and shifts in consumer preferences, can influence the overall economic performance of the electricity sector. The differential impact between rural and urban areas can be attributed to disparities in industry structures, labor market dynamics, and specific policy contexts. Considering the implications for factor income, the PTC policy positively impacts highly educated labor income, while low and medium-skilled labor may experience slight decreases. This finding underscores the need for policymakers to carefully consider the distributional impacts of renewable energy policies and explore ways to mitigate any adverse effects on low and medium-skilled workers.

These results suggest that implementing a production tax credit can lead to significant reductions in electricity prices and positive outcomes for the electricity and agricultural sectors. However, policymakers should carefully consider the unique characteristics of the electricity market, distributional impacts on different income groups, and the evolving dynamics of the renewable energy sector to ensure a balanced and inclusive transition towards sustainable energy systems.

Bibliography

Al-Riffai, P., Blohmke, J., Breisinger, C., and Wiebelt, M. (2015). Harnessing the sun and wind for economic development? an economy-wide assessment for egypt. *Sustainability*, 7(6):7714–7740.

Antweiler, W. (2021). Microeconomic models of electricity storage: Price forecasting, arbitrage limits, curtailment insurance, and transmission line utilization. *Energy Economics*, 101:105390.

Badea, L. and Mungiu-Pupazan, M. C. (2021). The economic and environmental impact of bitcoin. *IEEE access*, 9:48091–48104.

Böhringer, C., Keller, A., and Van der Werf, E. (2013). Are green hopes too rosy? employment and welfare impacts of renewable energy promotion. *Energy Economics*, 36:277–285.

Bourguignon, F. and Bussolo, M. (2013). Income distribution in computable general equilibrium modeling. *Handbook of computable general equilibrium modeling*, 1:1383–1437.

Burkhardt, J., Gillingham, K., and Kopalle, P. K. (2019). Experimental evidence on the effect of information and pricing on residential electricity consumption. Technical report, National Bureau of Economic Research.

Cai, Y. and Arora, V. (2015). Disaggregating electricity generation technologies in cge models: A revised technology bundle approach with an application to the us clean power plan. *Applied energy*, 154:543–555.

Cai, Y., Newth, D., Finnigan, J., and Gunasekera, D. (2015). A hybrid energy-economy model for global integrated assessment of climate change, carbon mitigation and energy transformation. *Applied Energy*, 148:381–395.

Delgado-Mohatar, O., Felis-Rota, M., and Fernández-Herraiz, C. (2019). The bitcoin mining breakdown: Is mining still profitable? *Economics Letters*, 184:108492.

Fell, H., Kaffine, D. T., and Novan, K. (2021). Emissions, transmission, and the environmental value of renewable energy. *American Economic Journal: Economic Policy*, 13(2):241–272.

Freire-González, J. and Puig-Ventosa, I. (2019). Reformulating taxes for an energy transition. *Energy Economics*, 78:312–323.

Garratt, R. and van Oordt, M. R. (2020). Why fixed costs matter for proof-of-work based cryptocurrencies. *Available at SSRN 3572400*.

Hannum, C., Cutler, H., Iverson, T., and Keyser, D. (2017). Estimating the implied cost of carbon in future scenarios using a cge model: The case of colorado. *Energy Policy*, 102:500–511.

Hanoch, G. (1971). Cresh production functions. *Econometrica: Journal of the Econometric Society*, pages 695–712.

Horridge, M. (2000). *ORANI-G: A general equilibrium model of the Australian economy*. Centre of Policy Studies (CoPS).

Hwang, W.-S. and Lee, J.-D. (2015). A cge analysis for quantitative evaluation of electricity market changes. *Energy Policy*, 83:69–81.

Isdinarmiati, T. and Oktaviani, R. (2012). Kenaikan tarif dasar listrik dan respon kebijakan untuk meminimisasi dampak negatif terhadap perekonomian. *Jurnal ekonomi dan kebijakan pembangunan*, 1(1):29–42.

Jiang, S., Li, Y., Lu, Q., Hong, Y., Guan, D., Xiong, Y., and Wang, S. (2021). Policy assessments for the carbon emission flows and sustainability of bitcoin blockchain operation in china. *Nature communications*, 12(1):1–10.

Johansson, V. and Göransson, L. (2020). Impacts of variation management on cost-optimal investments in wind power and solar photovoltaics. *Renewable Energy Focus*, 32:10–22.

Keyser, D., Cutler, H., Rose, A., Wei, D., and Shields, M. (2021). The los angeles 100% renewable energy study (la100): Chapter 11. economic impacts and jobs.

Lantz, E. (2009). Economic development benefits from wind energy in nebraska: A report for the nebraska energy office (revised). Technical report, National Renewable Energy Lab.(NREL), Golden, CO (United States).

McKibbin, W. J. and Wilcoxen, P. J. (1999). The theoretical and empirical structure of the g-cubed model. *Economic modelling*, 16(1):123–148.

Oei, P.-Y., Brauers, H., and Herpich, P. (2020). Lessons from germany's hard coal mining phase-out: policies and transition from 1950 to 2018. *Climate Policy*, 20(8):963–979.

Panhans, M., Lavric, L., and Hanley, N. (2017). The effects of electricity costs on firm re-location decisions: insights for the pollution havens hypothesis? *Environmental and Resource Economics*, 68:893–914.

Papageorgiou, O., Sedlmeir, J., Fridgen, G., Vlachos, I., Kostopoulos, N., Damvakeraki, T., Noszek, Z., Papoutsoglou, I., Anania, A., Belotti, M., et al. (2021). Energy efficiency of blockchain technologies. European Union Blockchain Observatory & Forum.

Prat, J. and Walter, B. (2021). An equilibrium model of the market for bitcoin mining. *Journal of Political Economy*, 129(8):2415–2452.

Schinckus, C. (2021). Proof-of-work based blockchain technology and anthropocene: An undermined situation? *Renewable and Sustainable Energy Reviews*, 152:111682.

Seel, J., Millstein, D., Mills, A., Bolinger, M., and Wiser, R. (2021). Plentiful electricity turns wholesale prices negative. *Advances in Applied Energy*, 4:100073.

Soummane, S., Ghersi, F., and Lefèvre, J. (2019). Macroeconomic pathways of the saudi economy: The challenge of global mitigation action versus the opportunity of national energy reforms. *Energy Policy*, 130:263–282.

Stoll, C., Klaaßen, L., and Gallersdörfer, U. (2019). The carbon footprint of bitcoin. *Joule*, 3(7):1647–1661.

Wang, Y., Yan, W., Zhuang, S., and Zhang, Q. (2019). Competition or complementarity? the hydropower and thermal power nexus in china. *Renewable Energy*, 138:531–541.

Winton, B. (2021). Solar + battery + bitcoin mining.

Yusuf, A. A. and Resosudarmo, B. P. (2008). Mitigating distributional impact of fuel pricing reform: the indonesian experience. *ASEAN Economic Bulletin*, 25(1):32–47.